Iranian Journal of Numerical Analysis and Optimization
Vol. 13, No. 3, 2023, pp 397–425
https://doi.org/10.22067/ijnao.2023.80916.1215
https://ijnao.um.ac.ir/

How to cite this article
Research Article

Solving two-dimensional coupled Burgers equations via a stable hybridized discontinuous Galerkin method

S. Baharlouei, R. Mokhtari*, and N. Chegini

Abstract

The purpose of this paper is to design a fully discrete hybridized discontinuous Galerkin (HDG) method for solving a system of two-dimensional (2D) coupled Burgers equations over a specified spatial domain. The semi-discrete HDG method is designed for a nonlinear variational formulation on the spatial domain. By exploiting broken Sobolev approximation spaces in the HDG scheme, numerical fluxes are defined properly. It is shown that the proposed method is stable under specific mild conditions on the stabilization parameters to solve a well-posed (in the sense of energy method) 2D coupled Burgers equations, which is imposed by Dirichlet boundary conditions. The fully discrete HDG scheme is designed by exploiting the Crank–Nicolson method for time discretization. Also, the Newton–Raphson method that has the order of at least two is nominated for solving the obtained nonlinear system of coupled Burgers equations over the rectangular domain. To reduce the complexity of the proposed method and the size of the linear system, we exploit the Schur complement idea. Numerical results declare that the best possible rates of convergence are achieved for approximate solutions of the 2D coupled Burgers equations and their first-order derivatives. Moreover, the proposed HDG method is examined for two other types of systems, that is, a system with high Reynolds numbers and a system with an unavailable exact solution. The acceptable results

*Corresponding author

Received 2 February 2023; revised 5 April 2023; accepted 10 April 2023

Shima Baharlouei
Department of Mathematical Sciences, Isfahan University of Technology, Isfahan 84156-83111, Iran.. e-mail: s.baharloui@math.iut.ac.ir

Reza Mokhtari
Department of Mathematical Sciences, Isfahan University of Technology, Isfahan 84156-83111, Iran. e-mail: mokhtari@iut.ac.ir

Nabi Chegini
Department of Mathematics, Tafresh University, Tafresh 39518-79611, Iran. e-mail: nabichegini@tafreshu.ac.ir

of examples show the flexibility of the proposed method in solving various problems.

AMS subject classifications (2020): 65M60, 65M12

Keywords: Coupled Burgers equations; hybridized discontinuous Galerkin method; stability analysis.

1 Introduction

Throughout the history of science, finding the analytical and especially numerical solutions of nonlinear evolution equations such as Burgers and coupled Burgers equations [3, 28, 31, 35], KdV type equations [2, 4, 27], Navier–Stokes equations [34], and nonlinear Schrödinger equations [7] play crucial roles in various fields of science and engineering for the detection of physical phenomena. The system of two-dimensional (2D) coupled Burgers equations, as a simplified form of some complex and practical equations in engineering such as the incompressible Navier-Stokes equation, is widely used in fluid dynamics such as modeling of the shock waves moving in viscous liquid [17], shallow water waves [18, 26], turbulent medium [5], and diffusion processes [1]. According to the new works that are done in the literature [24, 38, 39], we realize that providing methods of finding the numerical solutions of Burgers and coupled Burgers equations still have their importance. Moreover, numerical scientists consider Burgers and coupled Burgers equations as test problems to introduce and experiment with new numerical methods. In other words, these equations are used to compare different numerical methods in various aspects to choose and extend the most appropriate one to a specialized subject. This paper proposes a stable scheme for solving the 2D nonlinear coupled Burgers equations over rectangular domains numerically.

The general form of the 2D system of coupled Burgers equations reads as

$$\begin{cases} \mathfrak{u}_t + \mathfrak{u}\mathfrak{u}_x + \mathfrak{v}\mathfrak{u}_y - \dfrac{1}{\mathrm{Re}}(\mathfrak{u}_{xx} + \mathfrak{u}_{yy}) = 0, \\ \mathfrak{v}_t + \mathfrak{u}\mathfrak{v}_x + \mathfrak{v}\mathfrak{v}_y - \dfrac{1}{\mathrm{Re}}(\mathfrak{v}_{xx} + \mathfrak{v}_{yy}) = 0, \end{cases}$$

or equivalently

$$\begin{cases} \mathfrak{u}_t + \mathbf{U}\cdot\nabla\mathfrak{u} - \dfrac{1}{\mathrm{Re}}\Delta\mathfrak{u} = 0, \\ \mathfrak{v}_t + \mathbf{U}\cdot\nabla\mathfrak{v} - \dfrac{1}{\mathrm{Re}}\Delta\mathfrak{u} = 0, \end{cases} \tag{1}$$

where $\mathrm{Re} > 0$ is the Reynolds number, $\mathbf{U} = (\mathfrak{u}, \mathfrak{v})^\intercal$, and $\mathbf{x} = (x, y) \in \Omega = (a, b) \times (c, d) \subset \mathbb{R}^2$. In this paper, system (1) is equipped by the Dirichlet boundary conditions and suitable initial conditions.

Analytical solution of system (1) can be obtained, for instance, by the Hopf–Cole transformation; see [20]. Providing an explicit analytical solution for system (1) is not trivial. However, if, by any chance, an explicit form becomes available, then evaluating the analytical solution requires high computational costs with a considerable amount of time, which may be accompanied by uncontrollable errors regarding the discretization of the analytical solution. Based on these reasons, it is requested design be stable and effective numerical methods for computing numerical solutions. For solving system (1), many numerical methods have been proposed, such as the decomposition method [19], Chebyshev spectral collocation method [23], and some others; for instance, see [24, 38, 39].

Since the main approach of this paper is directly related to the discontinuous Galerkin (DG) method and is considered a continuation of the local discontinuous Galerkin (LDG) method, it is necessary to briefly review the history and background of DG and LDG methods. The first DG method was proposed by Reed and Hill in 1973 for a time-independent linear hyperbolic equation [6], and then it was utilized and developed for time-dependent partial differential equations (PDEs); see [10, 16]. Provable cell-entropy inequality for L^2 stability, h-p adaptivity, and flexibility to handle complicated geometry for arbitrary order of accuracy with local in-data communication, and other abilities lead to applying the DG method to various types of differential equations. To dominate the limitations of the DG method for solving high-order partial differential equations, an LDG method was proposed. This method was used for the first time for solving a second-order time-dependent convection-diffusion equation [15]. The main idea of the LDG method is the transformation of a high-order equation into a first-order system of equations before solving the new system by the DG method. Due to eliminating all of the auxiliary variables locally, the LDG method inherits all flexibilities of the DG method. Recent applications of the LDG method for higher-order nonlinear PDEs can be found, for instance, in [8, 25, 31].

The usage of the hybridization technique in the context of the finite element method goes back many years ago, while its application in the context of DG methods has a recent history and goes back to 2004. In fact, the hybridized discontinuous Galerkin (HDG) method was proposed for the first time by combining the DG method and continuous Galerkin (CG) method to solve the steady-state problems [11], and then it was generalized by Cockburn et al. [12, 13, 14]. Recently, HDG methods have been widely used to solve evolution equations numerically, in particular for compressible flow problems [22, 30, 33, 36, 37], Stokes flow [9, 21], continuum mechanics problems [29], and linear elasticity problems [32]. The HDG methods inherit the optimal convergence rate from the DG methods for approximate solutions and their derivatives with respect to spatial variables. HDG methods have two kinds of unknowns; global unknowns that are used in the definition of numerical traces (or in numerical fluxes) and obtained from the global system, and local unknowns that can be eliminated locally and are obtained by weak formula-

tion. Local and global unknowns are approximated by piecewise polynomials of degree k, respectively, in $\mathbb{R}^d$ and $\mathbb{R}^{d-1}$, where d is the dimension of the spatial domain. Due to the consideration of global unknowns, one can infer that the degree of freedom in the HDG method is reduced compared to the traditional implicit DG methods. The key to the success of the HDG method is the way of defining numerical fluxes that are based on global unknowns and stabilization parameters. The numerical fluxes of the HDG method are not defined uniquely in most situations, but those have to be defined in such a way that the desired definitions of numerical fluxes ensure the stability of the scheme. Also, the definitions of the numerical fluxes cause significantly smaller bandwidth than the corresponding matrices of the traditional CG method, and therefore lower computational cost is accessible in any HDG method. In solving a problem with nonsmooth solutions, the HDG method as a kind of DG method is a suitable scheme. This advantage is based on the fact that the HDG method produces numerical approximations using discontinuous trial functions over the entire given domain. In summary, it is worth pointing out that the HDG method has unique properties, which make this method superior, such as reducing the degree of freedom compared to the traditional implicit DG methods, making smaller bandwidth compared to the corresponding matrices of traditional CG and DG methods, and having less computational time; see [4]. In this paper, we intend to use a kind of HDG method for discretizing the 2D coupled Burgers equations (1) in the spatial domain.

The rest of the paper is organized as follows. In Section 2, some prerequisites such as notations, discretization of temporal and spatial domains, and approximation spaces, are expressed in dimension two. Section 3 is dedicated to the employment of the HDG method to the 2D coupled Burgers equations. In fact, in this section, a semi-discrete scheme is presented for the 2D coupled Burgers equations with suitable definitions of numerical fluxes and stabilization parameters. In addition, the stability of the proposed semi-discrete HDG scheme is investigated in this section. In other words, we prove that the method is stable in the L^2 norm under certain conditions on the stabilization parameters. Then, a full discretization approach is designed in Section 4 by exploiting the Crank–Nicolson method for time discretization and Newton–Raphson as a nonlinear solver. Numerical experiments in Section 5 show that the optimal order of accuracy is derived by the proposed method. Also, by performing some experiments, the numerical solutions of system (1) are investigated for large Reynolds numbers. Moreover, a 2D problem with different values of Reynolds numbers is investigated such that its exact solution is unavailable. The conclusion is given in Section 6. The paper is ended with an Appendix.

2 Prerequisites

Order to set up a system of weak formulation of coupled Burgers equations, it requires defining necessary notations and relevant approximation spaces for a desired HDG method. With T as a final time and for all $t \in (0, T]$, we consider a given bounded spatial domain $\Omega \subset \mathbb{R}^2$ with suitable partitioning. Suppose that the domain $\Omega = (a, b) \times (c, d)$ is split into conforming and uniform finite element meshes with N triangles such that in this mesh generation, all triangles have no intersection except in common edges or vertices. In general, each of these triangles is denoted by $\mathcal{K}$. By considering h as the longest edge among triangles, the finite collection of disjoint elements, and the set of the boundaries of elements, respectively, are denoted by

$$\mathscr{K}_h := \{\mathcal{K}\}, \qquad \partial\mathscr{K}_h = \{\partial\mathcal{K}\},$$

where $\Omega = \bigcup_{\mathcal{K}\in\mathscr{K}_h} \mathcal{K}$, and $\partial\mathcal{K}$ denotes the boundary of element $\mathcal{K}$. The collection $\mathcal{F}_h = \mathcal{F}_h^{\partial} \cup \mathcal{F}_h^0$ is the set of all faces such that $\mathcal{F}_h^0$ and $\mathcal{F}_h^{\partial}$ represent, respectively, the set of interior and boundary faces. More precisely, the set of faces contains all edges of triangles. Let us consider two elements $\mathcal{K}^-$ and $\mathcal{K}^+$ and their common face $e = \partial\mathcal{K}^- \cap \partial\mathcal{K}^+ \in \mathcal{F}_h^0$. As illustrated in Figure 1, $\mathbf{n}^-$ and $\mathbf{n}^+$ are, respectively, the corresponding outward unit normal vectors of face e with respect to $\mathcal{K}^-$ and $\mathcal{K}^+$. Let v^- and v^+ be the limits of the function v at face e associated with $\partial\mathcal{K}^+$ and $\partial\mathcal{K}^-$, respectively. Thus the mean and jump values of an arbitrary real valued function v on the given face e are, respectively, defined as

$$\{\{v\}\} = \frac{1}{2}(v^- + v^+), \quad [[v]] = v^-\mathbf{n}^- + v^+\mathbf{n}^+.$$

We note that the mean and jump values of function v at boundary face

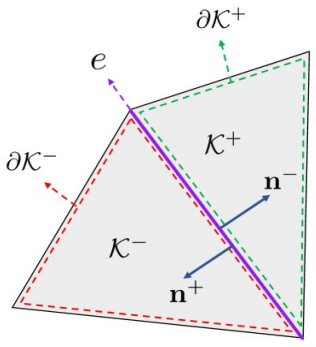

Figure 1: Common face e of two elements $\mathcal{K}^+, \mathcal{K}^-$ with outward unit vectors.

$e = \partial\Omega \cap \mathcal{K} \in \mathcal{F}_h^\partial$ are determined as $\{\{v\}\} = v$ and $[[v]] = v\mathbf{n}$, respectively. So, the mean and jump of function v can be rewritten as

$$\{\{v\}\} = \begin{cases} (v^+ + v^-)/2, & e \in \mathcal{F}_h^0, \\ v, & e \in \mathcal{F}_h^\partial, \end{cases} \qquad [[v\mathbf{n}]] = \begin{cases} v^+\mathbf{n}^+ + v^-\mathbf{n}^-, & e \in \mathcal{F}_h^0, \\ v\mathbf{n}, & e \in \mathcal{F}_h^\partial. \end{cases}$$

To obtain weak formulations of the 2D coupled Burgers equations, one needs to define appropriate approximation spaces. Regarding the nature of any DG method, broken Sobolev spaces are relevant spaces for approximating the solutions of system (1) via the HDG method. The corresponding broken Sobolev space, associated with the partition $\mathscr{K}_h$ is defined as

$$H^1(\mathscr{K}_h) = \{v : \Omega \to \mathbb{R} : v\,|_{\mathcal{K}} \in H^1(\mathcal{K}), \text{for all } \mathcal{K} \in \mathscr{K}_h\},$$

and associated with the set $\mathcal{F}_h$ is defined as

$$\mathcal{M}^1(\mathcal{F}_h) = \{\mu : \mathcal{F}_h \to \mathbb{R} : \mu\,|_e \in H^1(e), \text{for all } e \in \mathcal{F}_h\}.$$

Discontinuous finite element spaces for scalar and vector valued functions, as subspaces of broken Sobolev space $H^1(\mathscr{K}_h)$ are, respectively, defined by

$$S_{h,k} = \Big\{w \in H^1(\mathscr{K}_h) : w\,|_{\mathcal{K}} \in \mathcal{P}_k(\mathcal{K}), \text{for all } \mathcal{K} \in \mathscr{K}_h\Big\},$$
$$\mathbf{S}_{h,k} = \Big\{w \in (H^1(\mathscr{K}_h))^2 : w\,|_{\mathcal{K}} \in (\mathcal{P}_k(\mathcal{K}))^2, \text{for all } \mathcal{K} \in \mathscr{K}_h\Big\},$$

where $\mathcal{P}_k(\mathcal{K})$ is the set of polynomials of degree at most k on the element $\mathcal{K} \in \mathscr{K}_h$. The approximation space of the broken Sobolev space over $\mathcal{F}_h$ (or skeleton space) is defined as

$$M_{h,k} = \{\mu \in \mathcal{M}^1(\mathcal{F}_h) : \mu\,|_e \in \mathcal{P}_k(e), \text{for all } e \in \mathcal{F}_h\}.$$

Regarding the boundary conditions, it is needed to define the appropriate subspace of the skeleton space. Consider Dirichlet boundary conditions and the boundary data $b_{\mathfrak{u}}$ and $b_{\mathfrak{v}}$ on $\partial\Omega$, which are associated with $\mathfrak{u}$ and $\mathfrak{v}$, respectively. Let $\Gamma_{\mathfrak{u}}$ and $\Gamma_{\mathfrak{v}}$ be collections of boundary faces in which boundary data $b_{\mathfrak{u}}$ and $b_{\mathfrak{v}}$ are specified over $\Gamma_{\mathfrak{u}}$ and $\Gamma_{\mathfrak{v}}$, respectively. Based on the given boundary conditions, we define

$$M_{h,k}(l, \Gamma) := \{\mu \in M_{h,k} : \mu(\mathbf{x}) = \Pi l(\mathbf{x}),\ \mathbf{x} \in \Gamma\},$$

where $\Gamma \in \{\Gamma_{\mathfrak{u}}, \Gamma_{\mathfrak{v}}\}$, and Π is the L^2 projection with respect to the skeleton space of the boundary of the domain Ω. The approximation spaces $S_{h,k}$, $\mathbf{S}_{h,k}$, and $M_{h,k}$ are equipped by the following inner products, respectively,

$$(w_1, w_2)_{\mathscr{K}_h} = \sum_{\mathcal{K} \in \mathscr{K}_h} (w_1, w_2)_{\mathcal{K}}, \quad \langle \mu_1, \mu_2 \rangle_{\partial\mathscr{K}_h} = \sum_{\mathcal{K} \in \mathscr{K}_h} \langle \mu_1, \mu_2 \rangle_{\partial\mathcal{K}},$$

where

$$(w_1, w_2)_{\mathcal{K}} = \int_{\mathcal{K}} w_1(\mathbf{x}) \cdot w_2(\mathbf{x})\ d\mathbf{x}, \quad \langle \mu_1, \mu_2 \rangle_{\partial\mathcal{K}} = \int_{\partial\mathcal{K}} \mu_1 \cdot \mu_2\ ds,$$

in which $w_1,\ w_2$ are defined on $\mathscr{K}_h$ and $\mu_1,\ \mu_2$ are defined on $\partial\mathscr{K}_h$. By considering vector functions $\boldsymbol{w} = (w_1, w_2)^\intercal$, $\boldsymbol{z} = (z_1, z_2)^\intercal$, $\boldsymbol{\mu} = (\mu_1, \mu_2)^\intercal$, and $\boldsymbol{\eta} = (\eta_1, \eta_2)^\intercal$, the following inner products are needed

$$(\boldsymbol{w}, \boldsymbol{z})_{\mathscr{K}_h} = \sum_{\mathcal{K} \in \mathscr{K}_h} (\boldsymbol{w}, \boldsymbol{z})_{\mathcal{K}}, \quad \langle \boldsymbol{\mu}, \boldsymbol{\eta} \rangle_{\partial\mathscr{K}_h} = \sum_{\mathcal{K} \in \mathscr{K}_h} \langle \boldsymbol{\mu}, \boldsymbol{\eta} \rangle_{\partial\mathcal{K}},$$

where $w_1,\ w_2,\ z_1$, and z_2 are defined on $\mathscr{K}_h$, and $\mu_1,\ \mu_2,\ \eta_1$, and η_2 are defined on $\partial\mathscr{K}_h$. Besides, we have

$$(\boldsymbol{w}, \boldsymbol{z})_{\mathcal{K}} = ((w_1, z_1)_{\mathcal{K}},\ (w_2, z_2)_{\mathcal{K}})^\intercal, \qquad \langle \boldsymbol{\mu}, \boldsymbol{\eta} \rangle_{\partial\mathcal{K}} = (\langle \mu_1, \eta_1 \rangle_{\partial\mathcal{K}}, \langle \mu_2, \eta_2 \rangle_{\partial\mathcal{K}})^\intercal.$$

3 Construction of the semi-discrete HDG method

As mentioned, we assume that system (1) is equipped by the Dirichlet boundary conditions over the rectangular domain Ω. The initial step is to reformulate the 2D coupled Burgers equations (1) into a first-order system of equations. By defining the auxiliary variables $\mathbf{P} = (\mathfrak{p}_1, \mathfrak{p}_2)^\intercal = (\nabla\mathfrak{u})^\intercal$ and $\mathbf{Q} = (\mathfrak{q}_1, \mathfrak{q}_2)^\intercal = (\nabla\mathfrak{v})^\intercal$, the corresponding first-order system of (1) reads as

$$\begin{cases} \mathfrak{u}_t + \mathbf{U} \cdot \nabla\mathfrak{u} - \dfrac{1}{\mathrm{Re}} \nabla \cdot \mathbf{P} = 0, \\ \mathbf{P} - \nabla\mathfrak{u} = 0, \\ \mathfrak{v}_t + \mathbf{U} \cdot \nabla\mathfrak{v} - \dfrac{1}{\mathrm{Re}} \nabla \cdot \mathbf{Q} = 0, \\ \mathbf{Q} - \nabla\mathfrak{v} = 0. \end{cases} \tag{2}$$

By establishing the corresponding semi-discrete HDG method of the system (2), the stability of the semi-discrete method over the temporal interval $[0, t]$ for $t \in (0, T]$, is explained in the next subsection.

To have a corresponding conditionally well-posed problem of the system (2), it is worth pointing out that this system should be equipped with initial and boundary conditions. Weak formulation of the system (2) can be formed by multiplying each equation of (2) by an appropriate test function, integrating over each element $\mathcal{K} \in \mathscr{K}_h$, and using the Green's first identity. Consequently, the aim is to find numerical approximations $(u, v, P, Q) \in S^2_{h,k} \times \mathbf{S}^2_{h,k}$ such that for all test functions $(w_1, w_2, \mathbf{w}_1, \mathbf{w}_2) \in S^2_{h,k} \times \mathbf{S}^2_{h,k}$ and $\mathcal{K} \in \mathscr{K}_h$, it holds that

$$\begin{cases} (u_t, w_1)_{\mathcal{K}} + (\mathbf{U}\cdot\nabla\mathbf{u}, w_1)_{\mathcal{K}} + (\frac{1}{\mathrm{Re}}P, \nabla w_1)_{\mathcal{K}} + \langle -\widehat{\frac{1}{\mathrm{Re}}P\mathbf{n}}, w_1\rangle_{\partial\mathcal{K}} = 0, \\ ((P, \mathbf{w}_1))_{\mathcal{K}} + ((u, \nabla\mathbf{w}_1))_{\mathcal{K}} - \langle\langle \hat{u}\mathbf{n}, \mathbf{w}_1\rangle\rangle_{\partial\mathcal{K}} = 0, \\ (v_t, w_2)_{\mathcal{K}} + (\mathbf{U}\cdot\nabla\mathfrak{v}, w_2)_{\mathcal{K}} + (\frac{1}{\mathrm{Re}}Q, \nabla w_2)_{\mathcal{K}} + \langle -\widehat{\frac{1}{\mathrm{Re}}Q\mathbf{n}}, w_2\rangle_{\partial\mathcal{K}} = 0, \\ ((Q, \mathbf{w}_2))_{\mathcal{K}} + ((v, \nabla\mathbf{w}_2))_{\mathcal{K}} - \langle\langle \hat{v}\mathbf{n}, \mathbf{w}_2\rangle\rangle_{\partial\mathcal{K}} = 0. \end{cases} \tag{3}$$

- Under imposed boundary conditions, numerical traces $\hat{u} \in M_{h,k}(b_{\mathfrak{u}}, \Gamma_{\mathfrak{u}})$ and $\hat{v} \in M_{h,k}(b_{\mathfrak{v}}, \Gamma_{\mathfrak{v}})$ are properly defined for all $z \in \mathcal{F}_h$ as

$$\hat{u}(z) = \begin{cases} b_{\mathfrak{u}},\ z \in \Gamma_{\mathfrak{u}}, \\ \xi,\ \ z \in \mathcal{F}_h \setminus \Gamma_{\mathfrak{u}}, \end{cases} \qquad \hat{v}(z) = \begin{cases} b_{\mathfrak{v}},\ z \in \Gamma_{\mathfrak{v}}, \\ \zeta,\ \ z \in \mathcal{F}_h \setminus \Gamma_{\mathfrak{v}}, \end{cases} \tag{4}$$

  where $(\xi, \zeta) \in M_{h,k}(0, \Gamma_{\mathfrak{u}}) \times M_{h,k}(0, \Gamma_{\mathfrak{v}})$ is a global unknown pair. It can be observed that boundary data $b_{\mathfrak{u}}$ and $b_{\mathfrak{v}}$ are imposed in the definitions of the numerical traces $\hat{u}$ and $\hat{v}$, respectively, on $\Gamma_{\mathfrak{u}}$ and $\Gamma_{\mathfrak{v}}$. One can infer that $\hat{u}$ and $\hat{v}$ are global unknowns corresponding to the faces without a defined boundary data.

- In order to guarantee the stability of the semi-discrete method, numerical fluxes $\widehat{-\frac{1}{\mathrm{Re}}P}$ and $\widehat{-\frac{1}{\mathrm{Re}}Q}$ are defined as

$$\widehat{-\frac{1}{\mathrm{Re}}P} = -\frac{1}{\mathrm{Re}}P + \tau(u - \hat{u})\mathbf{n}, \qquad \widehat{-\frac{1}{\mathrm{Re}}Q} = -\frac{1}{\mathrm{Re}}Q + \sigma(v - \hat{v})\mathbf{n}, \tag{5}$$

  where $\mathbf{n}$ is the outward unit normal vector with respect to the considered face. In (5), τ and σ are the stabilization parameters. The valid range of parameters τ and σ are determined in the stability theorem of the proceeding subsection. We note that the definitions of the numerical fluxes in (5) are not unique and depend on the form and physics of the problems.

Remark 1. It is noteworthy that numerical fluxes and stabilization parameters play a key role in the stability of the semi-discrete method. We emphasize that functions $-\frac{1}{\mathrm{Re}}P$ and $-\frac{1}{\mathrm{Re}}Q$ on each element edge are approximated by their corresponding numerical fluxes so that the numerical fluxes are single-valued continuous functions across the element edges. In HDG methods, numerical fluxes depend on the numerical traces while global unknowns in the definitions of numerical traces depend on the faces.

Due to the fact that $\hat{u}$ and $\hat{v}$ contain two global unknown variables over $[0, T] \times \Omega$, two extra global equations on each face should be added to the system (3). The required global equations can be gained by enforcing the conservation of the fluxes. Thus, the global unknowns are obtained with the following extra global equations:

$$[[\widehat{\frac{1}{\mathrm{Re}}P\cdot\mathbf{n}}]]=0,\quad \text{for}\quad \mathrm{e}\in\mathcal{F}_{\mathrm{h}}^{0},\qquad [[\widehat{\frac{1}{\mathrm{Re}}\mathrm{Q}\cdot\mathbf{n}}]]=0,\quad \text{for}\quad \mathrm{e}\in\mathcal{F}_{\mathrm{h}}^{0}. \tag{6}$$

Then the local unknowns u, v, P, and Q, can be found by solving weak formulation (3) in each element $\mathcal{K}\in\mathscr{K}_h$.

3.1 Stability analysis

In this subsection, we verify the numerical stability of the weak formulation (3) over the time interval $[0,t]$, for all $t\in(0,T]$. To do this, let homogeneous Dirichlet boundary conditions imposed to the weak formulation (3). We start the analysis by multiplying the first equation of (1) by $\mathfrak{u}$ to get

$$\frac{1}{2}\frac{d}{dt}\mathfrak{u}^2+\frac{1}{2}\mathbf{U}\cdot\nabla(\mathfrak{u}^2)-\frac{1}{\mathrm{Re}}\mathfrak{u}\Delta\mathfrak{u}=0. \tag{7}$$

By integrating (7) over the given domain Ω and using the Green's first identity, we get

$$\frac{1}{2}\frac{d}{dt}\int_{\Omega}\mathfrak{u}^2\,d\mathbf{x}+\frac{1}{2}\int_{\Omega}\mathbf{U}\cdot\nabla(\mathfrak{u}^2)\,d\mathbf{x}+\frac{1}{\mathrm{Re}}\int_{\Omega}\nabla\mathfrak{u}\cdot\nabla\mathfrak{u}\,d\mathbf{x}-\frac{1}{\mathrm{Re}}\int_{\Gamma}\mathfrak{u}\frac{\partial\mathfrak{u}}{\partial\mathbf{n}}\,ds=0. \tag{8}$$

By applying homogeneous Dirichlet boundary conditions to (8) and regarding $\displaystyle\int_{\Omega}\nabla\mathfrak{u}\cdot\nabla\mathfrak{u}\,d\mathbf{x}\geq 0$, one can conclude that (8) leads to

$$\frac{1}{2}\frac{d}{dt}\int_{\Omega}\mathfrak{u}^2\,d\mathbf{x}+\frac{1}{2}\int_{\Omega}\mathbf{U}\cdot\nabla(\mathfrak{u}^2)\,d\mathbf{x}\leq 0. \tag{9}$$

Integrating (9) over the time interval $[0,t]$, for $0<t\leq T$, the following inequality holds:

$$\|\mathfrak{u}(\cdot,t)\|_{\Omega}^2+\int_0^T\Phi(\mathfrak{u},\Omega)\,d\mathbf{x}\leq\|\mathfrak{u}(\cdot,0)\|_{\Omega}^2, \tag{10}$$

with

$$\Phi(\mathfrak{r},\Lambda)=\int_{\Lambda}\mathbf{U}\cdot\nabla(\mathfrak{r}^2)\,d\mathbf{x},$$

where $\mathfrak{r}$ is the function of $\mathbf{x}$ and t, and Λ is a subdomain of Ω. Also, Output of $\Phi(\mathfrak{r},\Lambda)$ is a function of variable t. In the same approach, from the second equation of (1), we get

$$\|\mathfrak{v}(\cdot,t)\|_{\Omega}^2+\int_0^T\Phi(\mathfrak{v},\Omega)\,dt\leq\|\mathfrak{v}(\cdot,0)\|_{\Omega}^2. \tag{11}$$

Theorem 1. Let weak formulation (3) be equipped by the homogeneous Dirichlet boundary conditions over the domain Ω. By assuming $\tau > 0$ and $\sigma > 0$, it can be proved that the solution of weak formulation (3) satisfies the following inequalities for all $t \in (0, T]$:

$$\|u(\cdot,t)\|^2_{\mathscr{K}_h} + \int_0^T \Phi(u, \mathscr{K}_h)\ dt \le \|u(\cdot,0)\|^2_{\mathscr{K}_h},$$
$$\|v(\cdot,t)\|^2_{\mathscr{K}_h} + \int_0^T \Phi(v, \mathscr{K}_h)\ dt \le \|v(\cdot,0)\|^2_{\mathscr{K}_h}.$$

Proof. By setting $w_1 = u$, $\mathbf{w}_1 = \frac{1}{\mathrm{Re}}P$, $w_2 = v$, and $\mathbf{w}_2 = \frac{1}{\mathrm{Re}}Q$, in the weak formulation (3) and summing the first three equations and the last three equations of (3) together, we get

$$\begin{aligned} &\frac{1}{2}\frac{d}{dt}\|u\|^2_{\mathcal{K}} + \frac{1}{\mathrm{Re}}\|P\|^2_{\mathcal{K}} + \bar{E}_{1,\mathcal{K}} + \frac{1}{2}\Phi(u,\mathcal{K}) = 0,\\ &\frac{1}{2}\frac{d}{dt}\|v\|^2_{\mathcal{K}} + \frac{1}{\mathrm{Re}}\|Q\|^2_{\mathcal{K}} + \bar{E}_{2,\mathcal{K}} + \frac{1}{2}\Phi(v,\mathcal{K}) = 0, \end{aligned} \tag{12}$$

where

$$\begin{aligned} \bar{E}_{1,\mathcal{K}} &= \tfrac{1}{\mathrm{Re}}(P,\nabla u)_{\mathcal{K}} + \tfrac{1}{\mathrm{Re}}(u,\nabla P)_{\mathcal{K}} + \langle \widehat{-\tfrac{1}{\mathrm{Re}}P}\cdot\mathbf{n}, u\rangle_{\partial\mathcal{K}} - \tfrac{1}{\mathrm{Re}}\langle \hat{u}\mathbf{n}, P\rangle_{\partial\mathcal{K}},\\ \bar{E}_{2,\mathcal{K}} &= \tfrac{1}{\mathrm{Re}}(Q,\nabla v)_{\mathcal{K}} + \tfrac{1}{\mathrm{Re}}(v,\nabla Q)_{\mathcal{K}} + \langle \widehat{-\tfrac{1}{\mathrm{Re}}Q}\cdot\mathbf{n}, v\rangle_{\partial\mathcal{K}} - \tfrac{1}{\mathrm{Re}}\langle \hat{v}\mathbf{n}, Q\rangle_{\partial\mathcal{K}}. \end{aligned}$$

Using the divergence theorem, the following relations are obtained:

$$\begin{aligned} \tfrac{1}{\mathrm{Re}}(P,\nabla u)_{\mathcal{K}} + \tfrac{1}{\mathrm{Re}}(u,\nabla P)_{\mathcal{K}} &= \tfrac{1}{\mathrm{Re}}\int_{\mathcal{K}}\nabla\cdot(Pu)\ dx = \tfrac{1}{\mathrm{Re}}\int_{\partial\mathcal{K}}(Pu)\cdot\mathbf{n}\ ds\\ &= \tfrac{1}{\mathrm{Re}}\langle P\cdot\mathbf{n}, u\rangle_{\partial\mathcal{K}},\\ \tfrac{1}{\mathrm{Re}}(Q,\nabla v)_{\mathcal{K}} + \tfrac{1}{\mathrm{Re}}(v,\nabla Q)_{\mathcal{K}} &= \tfrac{1}{\mathrm{Re}}\int_{\mathcal{K}}\nabla\cdot(Qv)\ dx = \tfrac{1}{\mathrm{Re}}\int_{\partial\mathcal{K}}(Qv)\cdot\mathbf{n}\ ds\\ &= \tfrac{1}{\mathrm{Re}}\langle Q\cdot\mathbf{n}, v\rangle_{\partial\mathcal{K}}, \end{aligned} \tag{13}$$

By applying (13) to $\bar{E}_{1,\mathcal{K}}$ and $\bar{E}_{2,\mathcal{K}}$, using

$$\langle \hat{u}\mathbf{n}, P\rangle_{\partial\mathcal{K}} = \langle P\cdot\mathbf{n}, \hat{u}\rangle_{\partial\mathcal{K}}, \qquad \langle \hat{v}\mathbf{n}, Q\rangle_{\partial\mathcal{K}} = \langle Q\cdot\mathbf{n}, \hat{v}\rangle_{\partial\mathcal{K}},$$

and adding

$$-\langle \widehat{-\frac{1}{\mathrm{Re}}P}\cdot\mathbf{n}, \hat{u}\rangle_{\partial\mathcal{K}} = 0, \qquad -\langle \widehat{-\frac{1}{\mathrm{Re}}Q}\cdot\mathbf{n}, \hat{v}\rangle_{\partial\mathcal{K}} = 0,$$

respectively, into $\bar{E}_{1,\mathcal{K}}$ and $\bar{E}_{2,\mathcal{K}}$, we obtain

$$\begin{aligned} \bar{E}_{1,\mathcal{K}} &= \langle \widehat{-\tfrac{1}{\mathrm{Re}}P}\cdot\mathbf{n}, u-\hat{u}\rangle_{\partial\mathcal{K}} + \langle \tfrac{1}{\mathrm{Re}}P\cdot\mathbf{n}, u-\hat{u}\rangle_{\partial\mathcal{K}}\\ &= \langle (\widehat{-\tfrac{1}{\mathrm{Re}}P} + \tfrac{1}{\mathrm{Re}}P)\cdot\mathbf{n}, u-\hat{u}\rangle_{\partial\mathcal{K}},\\ \bar{E}_{2,\mathcal{K}} &= \langle \widehat{-\tfrac{1}{\mathrm{Re}}Q}\cdot\mathbf{n}, v-\hat{v}\rangle_{\partial\mathcal{K}} + \langle \tfrac{1}{\mathrm{Re}}Q\cdot\mathbf{n}, v-\hat{v}\rangle_{\partial\mathcal{K}}\\ &= \langle (\widehat{-\tfrac{1}{\mathrm{Re}}Q} + \tfrac{1}{\mathrm{Re}}Q)\cdot\mathbf{n}, v-\hat{v}\rangle_{\partial\mathcal{K}}. \end{aligned}$$

Using the definitions of $\widehat{-\frac{1}{\mathrm{Re}}P}$ and $\widehat{-\frac{1}{\mathrm{Re}}Q}$ from (5), we obtain

$$\bar{E}_{1,\mathcal{K}} =< \tau, (u-\hat{u})^2 >_{\partial\mathcal{K}}, \qquad \bar{E}_{2,\mathcal{K}} =< \sigma, (v-\hat{v})^2 >_{\partial\mathcal{K}} .$$

By summing $\bar{E}_{1,\mathcal{K}}$ and $\bar{E}_{2,\mathcal{K}}$ over all elements, we get

$$\begin{aligned}\sum_{\mathcal{K}\in\mathscr{K}_h} \bar{E}_{1,\mathcal{K}} &= \sum_{\mathcal{K}\in\mathscr{K}_h} < \tau, (u-\hat{u})^2 >_{\partial\mathcal{K}} =< \tau, (u-\hat{u})^2 >_{\partial\mathscr{K}_h},\\ \sum_{\mathcal{K}\in\mathscr{K}_h} \bar{E}_{2,\mathcal{K}} &= \sum_{\mathcal{K}\in\mathscr{K}_h} < \sigma, (v-\hat{v})^2 >_{\partial\mathcal{K}} =< \sigma, (v-\hat{v})^2 >_{\partial\mathscr{K}_h} .\end{aligned}$$

According to the assumptions $\tau > 0$ and $\sigma > 0$, we can conclude $\sum_{\mathcal{K}\in\mathscr{K}_h} \bar{E}_{1,\mathcal{K}} \geq 0$ and $\sum_{\mathcal{K}\in\mathscr{K}_h} \bar{E}_{2,\mathcal{K}} \geq 0$. Finally, by summing (12) over all elements, using the obtained results, and $\|P\|^2_{\mathscr{K}_h}, \|Q\|^2_{\mathscr{K}_h} \geq 0$, we conclude

$$\frac{d}{dt}\|u\|^2_{\mathscr{K}_h} + \Phi(u,\mathscr{K}_h) \leq 0, \qquad \frac{d}{dt}\|v\|^2_{\mathscr{K}_h} + \Phi(v,\mathscr{K}_h) \leq 0.$$

By integrating above relations over $[0,t]$ for all $t \in (0,T]$, the assertion of the theorem is concluded. □

Remark 2. According to (10)–(11), by assuming

$$\int_0^T \Phi(\mathfrak{u},\Omega)\ dt \geq 0, \qquad \int_0^T \Phi(\mathfrak{v},\Omega)\ dt \geq 0,$$

one can verify that the 2D coupled Burgers equations (1) is well-posed in the sense of the energy method. Therefore, in this case and based on Theorem 1, the proposed HDG method is stable with $\tau > 0$ and $\sigma > 0$.

Briefly, Theorem 1 and Remark 2 show that the proposed semi-discrete HDG method is stable for solving well-posed 2D coupled Burgers equations provided some specific mild conditions on the stabilization parameters. Moreover, this stability is unconditional because we have no condition on the step sizes.

4 Numerical algorithm and implementation issues

In order to design a fully discrete approximation method for solving the 2D nonlinear coupled Burgers equations (1), it is needed to apply a time-discretization approach to the weak formulation (3). To do this, we simply use the Crank–Nicolson method which is a method of order two. By considering time step $\Delta t = \frac{T}{J}$ with $J \in \mathbb{N}$ and time level $t_n = n\Delta t$, for $n = 0,\ldots,J$, the weak formulation (3) changes to

$$\begin{cases} \frac{1}{\Delta t}(u^n, w_1)_{\mathcal{K}} + \frac{1}{2}(U^n \cdot \nabla \mathfrak{u}^n, w_1)_{\mathcal{K}} + \frac{1}{2}(\frac{1}{\mathrm{Re}} P^n, \nabla w_1)_{\mathcal{K}} + \frac{1}{2}\langle \widehat{(-\frac{1}{\mathrm{Re}} P)^n \mathbf{n}}, w_1 \rangle_{\partial\mathcal{K}} = l_1(w_1), \\ \qquad\qquad ((P^n, \mathbf{w}_1))_{\mathcal{K}} + ((u^n, \nabla \mathbf{w}_1))_{\mathcal{K}} - \langle\langle \hat{u}^n \mathbf{n}, \mathbf{w}_1 \rangle\rangle_{\partial\mathcal{K}} = 0, \\ \frac{1}{\Delta t}(v^n, w_2)_{\mathcal{K}} + \frac{1}{2}(U^n \cdot \nabla \mathfrak{v}^n, w_2)_{\mathcal{K}} + \frac{1}{2}(\frac{1}{\mathrm{Re}} Q^n, \nabla w_2)_{\mathcal{K}} + \frac{1}{2}\langle \widehat{(-\frac{1}{\mathrm{Re}} Q)^n \mathbf{n}}, w_2 \rangle_{\partial\mathcal{K}} = l_2(w_2), \\ \qquad\qquad ((Q^n, \mathbf{w}_2))_{\mathcal{K}} + ((v^n, \nabla \mathbf{w}_2))_{\mathcal{K}} - \langle\langle \hat{v}^n \mathbf{n}, \mathbf{w}_2 \rangle\rangle_{\partial\mathcal{K}} = 0, \end{cases} \tag{14}$$

where $U^n = (u^n, v^n)^\intercal$, $P^n = (p_1^n, p_2^n)^\intercal$, and $Q^n = (q_1^n, q_1^n)^\intercal$, and

$$\begin{aligned} l_1(w_1) &= \tfrac{1}{\Delta t}(u^{n-1}, w_1)_{\mathcal{K}} + \tfrac{1}{2}(U^{n-1} \cdot \nabla \mathfrak{u}^{n-1}, w_1)_{\mathcal{K}} + \tfrac{1}{2}(\tfrac{1}{\mathrm{Re}} P^{n-1}, \nabla w_1)_{\mathcal{K}} \\ &\quad + \tfrac{1}{2}\langle \widehat{(-\tfrac{1}{\mathrm{Re}} P)^{n-1} \mathbf{n}}, w_1 \rangle_{\partial\mathcal{K}}, \\ l_2(w_2) &= \tfrac{1}{\Delta t}(v^n, w_2)_{\mathcal{K}} + \tfrac{1}{2}(U^{n-1} \cdot \nabla \mathfrak{v}^{n-1}, w_2)_{\mathcal{K}} + \tfrac{1}{2}(\tfrac{1}{\mathrm{Re}} Q^{n-1}, \nabla w_2)_{\mathcal{K}} \\ &\quad + \tfrac{1}{2}\langle \widehat{(-\tfrac{1}{\mathrm{Re}} Q)^{n-1} \mathbf{n}}, w_2 \rangle_{\partial\mathcal{K}}. \end{aligned}$$

The superscripts n and $n-1$ stand for the values at the time levels t_n and t_{n-1}, respectively. Likewise, the global equations should be considered at the time level t_n. By summing over all elements, inserting the flux definitions (5) into (6) and (14) at the time level t_n and also using boundary conditions (4), the algebraic system of equations or vector-matrix system can be obtained. The obtained system, steamed by exploiting the Crank–Nicolson method, is nonlinear, and we intend to solve it numerically so that preserves the second-order convergence in the temporal domain. Nevertheless, we exploit the Newton–Raphson method for solving the obtained nonlinear system. We set

$$W^n = (u^n, v^n, p_1^n, p_2^n, q_1^n, q_2^n, \xi^n, \zeta^n) \in S_{h,k}^6 \times M_{h,k}(0, \Gamma_{\mathfrak{u}}) \times M_{h,k}(0, \Gamma_{\mathfrak{v}}),$$

where $(u^n, v^n, p_1^n, p_2^n, q_1^n, q_2^n, \xi^n, \zeta^n)$ is the exact solution vector of system (14) and (6) at the time level t_n. With a suitable initial guess $W_{n,0}$, we are aiming to generate the following sequence of solution vectors

$$W_{n,i} = W_{n,i-1} + \delta W_{n,i}, \quad i = 1, 2, \ldots,$$

where $W_{n,i}$ converges to the exact solution, namely, W^n, as i tends to infinity. We note that

$$\delta W_{n,i} = (\delta u_{n,i}, \delta v_{n,i}, \delta p_{1,n,i}, \delta p_{2,n,i}, \delta q_{1,n,i}, \delta q_{2,n,i}, \delta \xi_{n,i}, \delta \zeta_{n,i}),$$

is obtained via the Newton–Raphson method. In the other words, $\delta W_{n,i}$ is computed by solving the following linear variational formulation so that holds for all $(w_1, w_2, \mathbf{w}_1, \mathbf{w}_2) \in S_{h,k}^2 \times \mathbf{S}_{h,k}^2$ and $\mathcal{K} \in \mathscr{K}_h$ and $(\mu_1, \mu_2) \in M_{h,k}(0, \Gamma_{\mathfrak{u}}) \times M_{h,k}(0, \Gamma_{\mathfrak{v}})$:

$$\begin{aligned}
\tilde{\mathsf{a}}_1(\delta u_{n,i}, w_1) + \tilde{\mathsf{a}}_2(\delta v_{n,i}, w_1) + \tilde{\mathsf{a}}_3(\delta p_{1,n,i}, w_1) + \tilde{\mathsf{a}}_4(\delta p_{2,n,i}, w_1) \\
+\tilde{\mathsf{a}}_5(\delta \xi_{n,i}, w_1) = \tilde{\mathsf{l}}_1(w_1), \\
\tilde{\mathsf{b}}_1(\delta u_{n,i}, w_{11}) + \tilde{\mathsf{b}}_2(\delta p_{1,n,i}, w_{11}) + \tilde{\mathsf{b}}_3(\delta \xi_{n,i}, w_{11}) = \tilde{\mathsf{l}}_2(w_{11}), \\
\tilde{\mathsf{b}}_4(\delta u_{n,i}, w_{12}) + \tilde{\mathsf{b}}_2(\delta p_{2,n,i}, w_{12}) + \tilde{\mathsf{b}}_5(\delta \xi_{n,i}, w_{12}) = \tilde{\mathsf{l}}_3(w_{12}), \\
\tilde{\mathsf{c}}_1(\delta u_{n,i}, w_2) + \tilde{\mathsf{c}}_2(\delta v_{n,i}, w_2) + \tilde{\mathsf{c}}_3(\delta q_{1,n,i}, w_2) + \tilde{\mathsf{c}}_4(\delta q_{2,n,i}, w_2) \\
+\tilde{\mathsf{c}}_5(\delta \xi_{n,i}, w_2) = \tilde{\mathsf{l}}_4(w_2), \\
\tilde{\mathsf{b}}_1(\delta v_{n,i}, w_{21}) + \tilde{\mathsf{b}}_2(\delta q_{1,n,i}, w_{21}) + \tilde{\mathsf{b}}_3(\delta \zeta_{n,i}, w_{21}) = \tilde{\mathsf{l}}_5(w_{11}), \\
\tilde{\mathsf{b}}_4(\delta v_{n,i}, w_{22}) + \tilde{\mathsf{b}}_2(\delta q_{2,n,i}, w_{22}) + \tilde{\mathsf{b}}_5(\delta \zeta_{n,i}, w_{22}) = \tilde{\mathsf{l}}_6(w_{12}), \\
\tau\tilde{\mathsf{d}}_1(\delta u_{n,i}, \mu_1) + \tilde{\mathsf{d}}_2(\delta p_{1,n,i}, \mu_1) + \tilde{\mathsf{d}}_3(\delta p_{2,n,i}, \mu_1) - \tau\tilde{\mathsf{d}}_4(\delta \xi_{n,i}, \mu_1) = \tilde{\mathsf{l}}_7(\mu_1), \\
\sigma\tilde{\mathsf{d}}_1(\delta v_{n,i}, \mu_2) + \tilde{\mathsf{d}}_2(\delta q_{1,n,i}, \mu_2) + \tilde{\mathsf{d}}_3(\delta q_{2,n,i}, \mu_2) - \sigma\tilde{\mathsf{d}}_4(\delta \zeta_{n,i}, \mu_2) = \tilde{\mathsf{l}}_8(\mu_2).
\end{aligned} \tag{15}$$

where $\mathbf{w}_1 = (w_{11}, w_{12})^\intercal$, and $\mathbf{w}_2 = (w_{21}, w_{22})^\intercal$. To observe the definition of multilinear forms and linear functionals in (15), we refer the reader to Appendix of the paper.

In order to solve the large and sparse linear variational formulation (15) more effectively, this system can be decomposed into two linear systems with smaller sizes by using the Schur complement idea. One can observe that (15) can be reformulated to the following vector-matrix equations:

$$\begin{cases} M_{11}X_{n,i} + M_{12}Y_{n,i} = \mathcal{R}_1, \\ M_{21}X_{n,i} + M_{22}Y_{n,i} = \mathcal{R}_2, \end{cases} \tag{16}$$

where $X_{n,i} = [\delta\bar{u}_{n,i}\ \delta\bar{v}_{n,i}\ \delta\bar{p}_{1,n,i}\ \delta\bar{p}_{2,n,i}\ \delta\bar{q}_{1,n,i}\ \delta\bar{q}_{2,n,i}]^\intercal$, $Y_{n,i} = [\delta\bar{\xi}_{n,i}\ \delta\bar{\zeta}_{n,i}]^\intercal$ are coefficients of approximate solutions with

$$M_{11} = \begin{bmatrix} \tilde{A}_1 & \tilde{A}_2{}^\intercal & \tilde{A}_3 & \tilde{A}_4 & 0 & 0 \\ \tilde{B}_1 & 0 & \tilde{B}_2 & 0 & 0 & 0 \\ \tilde{B}_1 & 0 & 0 & \tilde{B}_2 & 0 & 0 \\ \tilde{C}_1 & \tilde{C}_2 & 0 & 0 & \tilde{C}_3 & \tilde{C}_4 \\ 0 & \tilde{B}_1 & 0 & 0 & \tilde{B}_2 & 0 \\ 0 & \tilde{B}_1 & 0 & 0 & 0 & \tilde{B}_2 \end{bmatrix}, \qquad M_{12} = \begin{bmatrix} \tilde{A}_5 & 0 \\ \tilde{B}_3 & 0 \\ \tilde{B}_4 & 0 \\ 0 & \tilde{C}_5 \\ 0 & \tilde{B}_3 \\ 0 & \tilde{B}_4 \end{bmatrix},$$

$$M_{22} = \begin{bmatrix} -\tau\tilde{D}_4 & 0 \\ 0 & -\sigma\tilde{D}_4 \end{bmatrix}, \qquad M_{21} = \begin{bmatrix} \tau\tilde{D}_1 & 0 & \tilde{D}_2 & \tilde{D}_3 & 0 & 0 \\ 0 & \sigma\tilde{D}_1 & 0 & 0 & \tilde{D}_2 & \tilde{D}_3 \end{bmatrix},$$

$$\mathcal{R}_1 = \begin{bmatrix} \tilde{L}_1 & \tilde{L}_2 & \tilde{L}_3 & \tilde{L}_4 & \tilde{L}_5 & \tilde{L}_6 \end{bmatrix}, \qquad \mathcal{R}_2 = \begin{bmatrix} \tilde{L}_7 & \tilde{L}_8 \end{bmatrix},$$

In the above matrices and vectors, capital letters are interpreted as the matrix and vector representation of multi-linear forms and linear functionals defined in (15). Based on our experiences in the computer implementation of the HDG method, we have not benefited by not encountering non-invertible matrix M_{11}. Regarding this fact, we assume that M_{11} is invertible. Otherwise, it is not possible to propose the reduction of the complexity of the computations for solving (15), and so this system has to be solved directly. Based on the structure of the matrices in vector-matrix equations (16) and

the Schur complement issue, instead of solving (16), the following system of equations are solved in each iteration of the Newton–Raphson method:

$$(M_{22} - M_{21}M_{11}^{-1}M_{12})Y_{n,i} = \mathcal{R}_2 - M_{21}M_{11}^{-1}\mathcal{R}_1. \tag{17}$$

Thus $X_{n,k}$ can be computed by

$$X_{n,i} = M_{11}^{-1}\mathcal{R}_1 - M_{11}^{-1}M_{12}Y_{n,i}. \tag{18}$$

Based on the Newton–Raphson approach, and Schur complement decomposition, we finish this section by representing the details of the designed HDG scheme in the following algorithm.

Algorithm *HDG algorithm for 2D coupled Burgers equations* (1)

Input: Spatial domain Ω and number of elements, namely, N, time interval $[0,T]$ and number of time steps J, degree of approximate polynomials k, boundary data $\Gamma_{\mathfrak{u}}$ and $\Gamma_{\mathfrak{v}}$, initial data, tolerance $0 < \epsilon$, and stabilization parameters τ and σ.

Output: u^J, v^J, p_1^J, p_2^J, q_1^J, q_2^J, ξ^J, and ζ^J that are the approximate solutions of $\mathfrak{u}(x,y,T)$, $\mathfrak{v}(x,y,T)$, $\mathfrak{p}_1(x,y,T)$, $\mathfrak{p}_2(x,y,T)$, $\mathfrak{q}_1(x,y,T)$, $\mathfrak{q}_2(x,y,T)$, $\xi(x,y,T)$ and $\zeta(x,y,T)$.

Generate regular mesh for the domain Ω.

Set W_0 *by given initial and boundary conditions.*

For $n = 1, 2, \ldots, J$ *do*

$W_{n,0} = W_{n-1},\ \delta W_{n,0} = (\epsilon + 1)\vec{1},\ i = 0.$

While $\epsilon < \|\delta W_{n,i}\|$ *do*

Compute $\delta W_{n,i+1}$ *by Schur complement formulas* (17) *and* (18)

$W_{n,i+1} = W_{n,i} + \delta W_{n,i+1},\ i = i + 1$

end While

$W^n = W_{n,i}$

end For

5 Numerical results

In this section, we aim to demonstrate the efficiency, validation, and applicability of the proposed fully discrete HDG method for system (1). We observe that the semi-discrete HDG method for system (1) is stable over the time interval $[0,t]$, for all $t \in (0,T]$ provided that system (1) is well-posed in

the sense of energy method. To design a fully discrete version of the HDG method, we proposed an approach with the order of at least two for time discretization, that is Crank–Nicolson. Also, the Newton–Raphson method that has the order of at least two is proposed for solving the obtained nonlinear system, and therefore, the loss of accuracy will not appear. As seen, to reduce the complexity of the proposed method and the size of the linear system, we exploited the Schur complement idea. Numerical experiments of the proposed HDG method are reported in three examples that they are selected from [35].

In Example 1, the 2D system (1) is considered to investigate the spatial order of accuracy of the proposed HDG method. Also, the results are reported for different Reynolds numbers. In Example 2, the HDG solution is examined for very high Reynolds numbers in the system (1). In Example 3, a 2D coupled Burgers equation without having any exact solution is solved. In this example, the HDG results are compared with the numerical results in [35] and [3].

Example 1. [35] Consider the 2D coupled Burgers equations (1) with $\Omega = (0,1)\times(0,1)$, $T = 1$, and the following exact solutions:

$$\mathfrak{u} = \frac{3}{4} - \frac{1}{4(1+\exp(\frac{\mathrm{Re}}{4}(-t-4x+4y)))},$$

$$\mathfrak{v} = \frac{3}{4} + \frac{1}{4(1+\exp(\frac{\mathrm{Re}}{4}(-t-4x+4y)))}.$$

The initial and boundary conditions can be derived from the exact solutions. In Table 1, L^2 error norms and corresponding orders are reported for $\mathrm{Re} = 1$ and $\tau = \sigma = 0.5$. As seen, satisfactory and high accuracy errors in Table 1 indicate the good performance of our proposed method in solving system (1). Moreover, the results show the optimal convergence for approximate solutions u, v, and their first derivatives. As mentioned earlier, this optimal convergence is inherited from the DG method that is preserved well by our proposed method. In Table 2, the errors are reported for different Reynolds numbers $\mathrm{Re} = 0.1, 1, 10, 100, 200, 500$, approximate polynomials of degree $k = 2$ and $h = 0.2$. For this test, we set $\tau = \sigma = 0.5$ for $\mathrm{Re} = 0.1, 1, 10, 100$ and $\tau = \sigma = 2$ for $\mathrm{Re} = 200, 500$. Note that, by increasing the Reynolds number, the effectiveness of dissipative terms in the system (1) will be eliminated gradually, and so we will face an inviscid system. Therefore, we expect that the accuracy of the method decreases as the Reynolds number increases. According to Table 2, we can observe that the proposed HDG method produces acceptable approximate solutions even for high Reynolds numbers and the reduction of accuracy is acceptable.

Here, we intend to do a test and check the dependence on the accuracy of the numerical solutions on the stability parameters. In Table 3, L^2 error norms and corresponding orders are reported for $\mathrm{Re} = 1$ and $\tau = \sigma = -0.5$.

Table 1: L^2 error norms of approximate solutions u, v, p_1, p_2, q_1, and q_2 together with their corresponding spatial orders of accuracy for Example 1 with $\mathrm{Re} = 1$, $\tau = \sigma = 0.5$ at $T = 1$.

k	h	$\|u - \mathfrak{u}\|_\Omega$	order	$\|p_1 - \mathfrak{p}_1\|_\Omega$	order	$\|p_2 - \mathfrak{p}_2\|_\Omega$	order
1	0.4	1.3059 E-6		3.7719 E-6		3.7620 E-6	
	0.2	3.2810 E-7	1.99	9.3005 E-7	2.02	9.3053 E-7	2.02
	0.1	7.6653 E-8	2.10	2.0728 E-7	2.017	2.0778 E-7	2.016
2	0.4	1.2004 E-6		3.8744 E-6		3.8762 E-6	
	0.2	1.5815 E-7	2.92	5.0946 E-7	2.93	5.0959 E-7	2.93
	0.1	1.9734 E-8	3.00	6.3571 E-8	3.00	6.3588 E-8	3.00
k	h	$\|v - \mathfrak{v}\|_\Omega$	order	$\|q_1 - \mathfrak{q}_1\|_\Omega$	order	$\|q_2 - \mathfrak{q}_2\|_\Omega$	order
1	0.4	1.3059 E-6		3.7719 E-6		3.7620 E-6	
	0.2	3.2810 E-7	1.99	9.3005 E-7	2.02	9.3053 E-7	2.02
	0.1	7.6653 E-8	2.10	2.0728 E-7	2.017	2.0778 E-7	2.016
2	0.4	1.2004 E-6		3.8744 E-6		3.8762 E-6	
	0.2	1.5815 E-7	2.92	5.0946 E-7	2.93	5.0959 E-7	2.93
	0.1	1.9734 E-8	3.00	6.3571 E-8	3.00	6.3588 E-8	3.00

Table 2: L^2 error norms for Example 1 with approximate polynomial of degree $k = 2$ and $h = 0.1$ for $\mathrm{Re} = 0.1, 1, 10, 100, 250$, and 500, at the final time $T = 1$.

Re	$\|u - \mathfrak{u}\|_\Omega$r	$\|p_1 - \mathfrak{p}_1\|_\Omega$	$\|p_2 - \mathfrak{p}_2\|_\Omega$	$\|v - \mathfrak{v}\|_\Omega$	$\|q_1 - \mathfrak{q}_1\|_\Omega$	$\|q_2 - \mathfrak{q}_2\|_\Omega$
0.1	1.6141 E-11	1.9859 E-10	1.9929 E-10	1.8628 E-11	2.7554 E-10	2.7644 E-10
1	1.2378 E-8	3.9750 E-8	3.9774 E-8	1.2378 E-8	3.9751 E-8	3.9772 E-8
10	6.7030 E-6	2.5580 E-5	2.6527 E-5	6.7030 E-6	2.5580 E-5	2.6527 E-5
100	1.0638 E-3	1.9183 E-2	2.1982 E-2	1.0638 E-3	1.9183 E-2	2.1982 E-2
200	3.3772 E-3	1.2515 E-1	1.3351 E-1	3.3773 E-3	1.2514 E-1	1.3351 E-1
500	2.1209 E-2	7.1691 E-1	6.9343 E-1	2.1210 E-2	7.1691 E-1	6.9343 E-1

We can observe that the HDG method with negative stabilization parameters produces numerical results with high and unacceptable errors.

Example 2. [35] The aim of this example is to investigate the performance of the HDG method in solving system (1) with high Reynolds numbers. Consider system (1) with $\Omega = (0,1) \times (0,1)$, $T = 1$, and exact solutions

$$\mathfrak{u} = -\frac{2\pi \exp(\frac{-5\pi^2 t}{\mathrm{Re}}) \cos(2\pi x) \sin(\pi y)}{\mathrm{Re}(2 + \exp(\frac{-5\pi^2 \mathrm{t}}{\mathrm{Re}}) \sin(2\pi \mathrm{x}) \sin(\pi \mathrm{y}))},$$

$$\mathfrak{v} = -\frac{2\pi \exp(\frac{-5\pi^2 t}{\mathrm{Re}}) \sin(2\pi x) \cos(\pi y)}{\mathrm{Re}(2 + \exp(\frac{-5\pi^2 \mathrm{t}}{\mathrm{Re}}) \sin(2\pi \mathrm{x}) \sin(\pi \mathrm{y}))}.$$

The errors of numerical solutions u and v are shown in Figures 2 and 3, respectively, for $Re = 10000$ and 100000. Note that, the results have been obtained by setting $\tau = \sigma = 20$, $h = 0.1$, and $k = 1$. As mentioned in

Table 3: L^2 error norms of approximate solutions u, v, p_1, p_2, q_1, and q_2 together with their corresponding spatial orders of accuracy for Example 1 with $\mathrm{Re} = 1$, $\tau = \sigma = -0.5$ at $T = 1$.

k	h	$\|u - \mathfrak{u}\|_\Omega$	order	$\|p_1 - \mathfrak{p}_1\|_\Omega$	order	$\|p_2 - \mathfrak{p}_2\|_\Omega$	order
1	0.4	7.2644		2.4545 E+1		2.3701 E+1	
	0.2	6.2532	0.22	1.4973 E+1	0.71	1.4567 E+1	0.70
	0.1	6.1053	0.03	1.4241 E+1	0.07	1.4304 E+1	0.03
2	0.4	2.9309 E+6		1.3503 E+5		1.6600 E+5	
	0.2	8.4685 E+6	-1.53	8.4199 E+5	-2.6	8.0063 E+5	-2.27
	0.1	2.2730 E+5	-1.42	5.4620 E+4	-2.70	4.6931 E+4	-2.55
k	h	$\|v - \mathfrak{v}\|_\Omega$	order	$\|q_1 - \mathfrak{q}_1\|_\Omega$	order	$\|q_2 - \mathfrak{q}_2\|_\Omega$	order
1	0.4	7.3625		2.6346 E+1		2.5501 E+1	
	0.2	6.2372	0.24	1.4836 E+1	0.83	1.4870 E+1	0.78
	0.1	6.0686	0.04	1.4378 E+1	0.05	1.4228 E+1	0.06
2	0.4	1.1331 E+6		5.3889 E+6		6.3966 E+6	
	0.2	5.2046 E+6	-2.20	5.1255 E+5	-3.25	4.9186 E+5	-2.94
	0.1	9.5820 E+6	-0.88	2.3339 E+4	-2.19	1.9896 E+4	-2.20

Example 1, these high Reynolds numbers are going to omit the dissipative terms in system (1), but we can infer from Figures 2 and 3 that the behaviors of approximate solutions still follow the exact solutions very well. This shows the flexibility and superiority of the proposed HDG method for solving different types of system (1) numerically.

Example 3. [3, 35] In this example, a 2D problem with different values of Reynolds numbers will be investigated such that its exact solution is unavailable. Consider the 2D coupled Burgers equations (1) over the domain $\Omega = (0, 0.5) \times (0, 0.5)$ with the initial conditions

$$\mathfrak{u}(x, y, 0) = \sin(\pi x) + \cos(\pi x) \qquad \mathfrak{v}(x, y, 0) = x + y,$$

and the boundary conditions

$$\begin{aligned}
&\mathfrak{u}(0, y, t) = \cos(\pi y), \quad \mathfrak{u}(0.5, y, t) = 1 + \cos(\pi y),\\
&\mathfrak{u}(x, 0, t) = 1 + \sin(\pi x), \quad \mathfrak{u}(x, 0.5, t) = \sin(\pi x),\\
&\mathfrak{v}(0, y, t) = y, \quad \mathfrak{v}(0.5, y, t) = 0.5 + y, \quad \mathfrak{v}(x, 0, t) = x, \quad \mathfrak{v}(x, 0.5, t) = 0.5 + x.
\end{aligned}$$

In the proposed HDG scheme, we set $\sigma = \tau = 2$, $h = 0.05$, $\Delta t = 0.001$, and $T = 0.625$. According to this system that has no available exact solution, the only way to understand the correctness of the results is the comparison them with the results of other papers. In the following, the results are compared with the results of [3, 35]. The numerical approximations u and v are illustrated in Figure 4 with $k = 2$ and $\mathrm{Re} = 50$. Also, in Tables 4 and 5, the numerical results are reported at some selected mesh points for $\mathrm{Re} = 50, 500$. We find that, the results of the proposed HDG method are in

Table 4: Comparison of computed values of u and v for $\mathrm{Re} = 50$ for Example 3. Results are reported for approximate polynomials of degree two, $h = 0.05$, and $\Delta t = 0.001$ at final time $T = 0.625$.

	u			v		
(x, y)	HDG method	[35]	[3]	HDG method	[35]	[3]
(0.1, 0.1)	0.96969	0.97146	0.96688	0.09817	0.09869	0.09824
(0.3, 0.1)	1.15072	1.15280	1.14827	0.14167	0.14158	0.14112
(0.2, 0.2)	0.86362	0.86307	0.85911	0.16915	0.16754	0.16681
(0.4, 0.2)	0.99136	0.97981	0.97637	0.18855	0.17109	0.17065
(0.1, 0.3)	0.66440	0.66316	0.66019	0.26491	0.26378	0.26261
(0.3, 0.3)	0.77587	0.77230	0.76932	0.24818	0.22654	0.22576
(0.2, 0.4)	0.59083	0.58180	0.57966	0.33124	0.32851	0.32745
(0.4, 0.4)	0.75273	0.75855	0.75678	0.38614	0.32499	0.32441

Table 5: Comparison of computed values of u and v for $\mathrm{Re} = 500$ for Example 3. Results are reported for approximate polynomials of degree two, $h = 0.05$, and $\Delta t = 0.001$ at final time $T = 0.625$.

	u			v		
(x, y)	HDG method	[35]	[3]	HDG method	[35]	[3]
(0.15, 0.1)	0.96114	0.96151	0.96650	0.08662	0.09230	0.09020
(0.3, 0.1)	0.97324	1.03200	1.02970	0.07841	0.10728	0.10690
(0.1, 0.2)	0.84445	0.87814	0.84449	0.17889	0.16816	0.17972
(0.2, 0.2)	0.86926	1.06370	0.87631	0.16264	0.23690	0.16777
(0.1, 0.3)	0.67883	0.67920	0.67809	0.26177	0.26268	0.26222
(0.3, 0.3)	0.77557	0.79947	0.79792	0.21739	0.23550	0.23497
(0.15, 0.4)	0.54874	0.58959	0.54601	0.31817	0.30419	0.31753
(0.2, 0.4)	0.58850	0.78233	0.58874	0.30049	0.35294	0.30371

good agreements with the presented results in [3, 35]. Hence, the proposed HDG method copes well with equations without the exact solution.

6 Discussion and conclusion

Numerical simulation of the 2D coupled Burgers equations via the HDG method has been studied in this paper, so that this system is equipped with appropriate initial and boundary conditions. In general, HDG methods have less computational time compared to the other DG methods, especially the LDG methods, which are the nearest to the HDG. The main reason for this advantage is the way of defining numerical fluxes. In the HDG method, the definition of numerical fluxes is not unique and depends on the form and physics of the problem. On the other hand, the stability of the method is

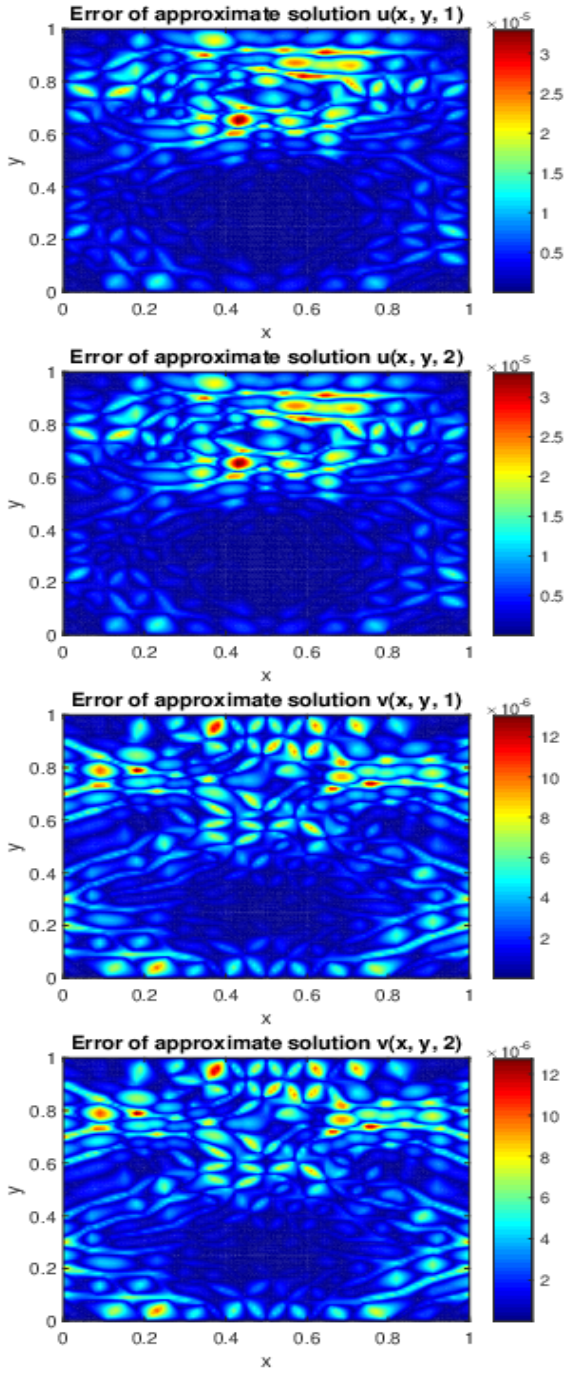

Figure 2: The errors of approximate solutions u and v for Example 2 with $Re = 10000$ at $T = 1, 2$. The results are reported for $\tau = \sigma = 20$, approximate polynomial of degree one, and $h = 0.1$.

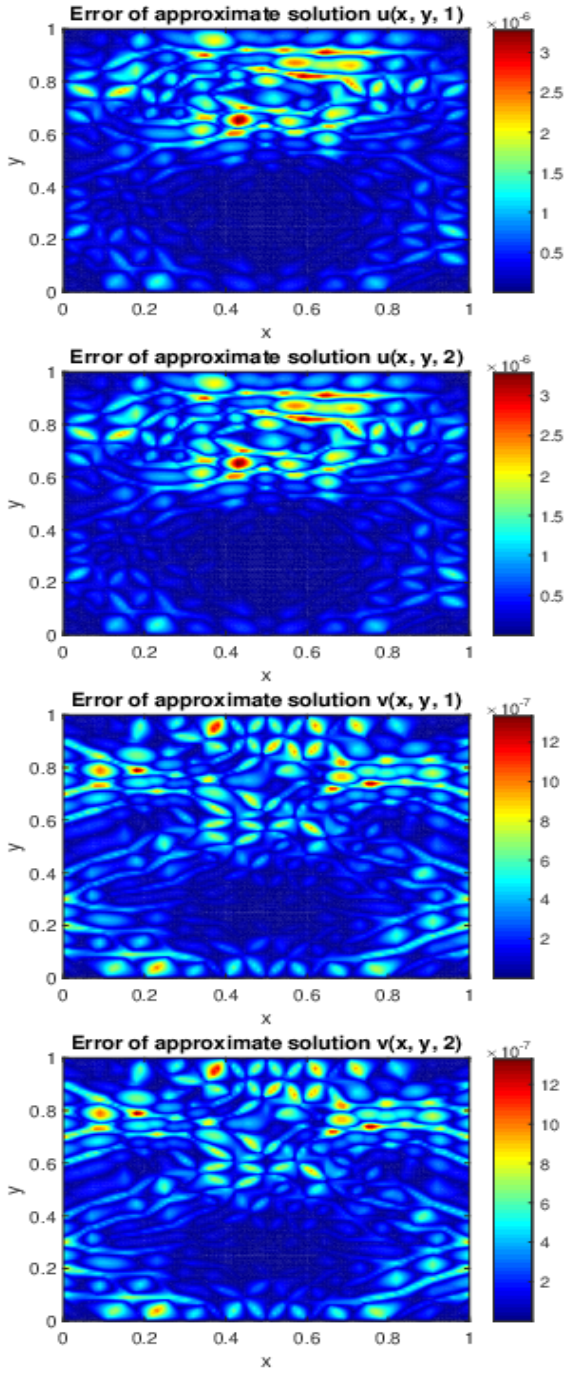

Figure 3: The errors of approximate solutions u and v for Example 2 with $Re = 100000$ at $T = 1, 2$. The results are reported for $\tau = \sigma = 20$, approximate polynomial of degree one, and $h = 0.1$.

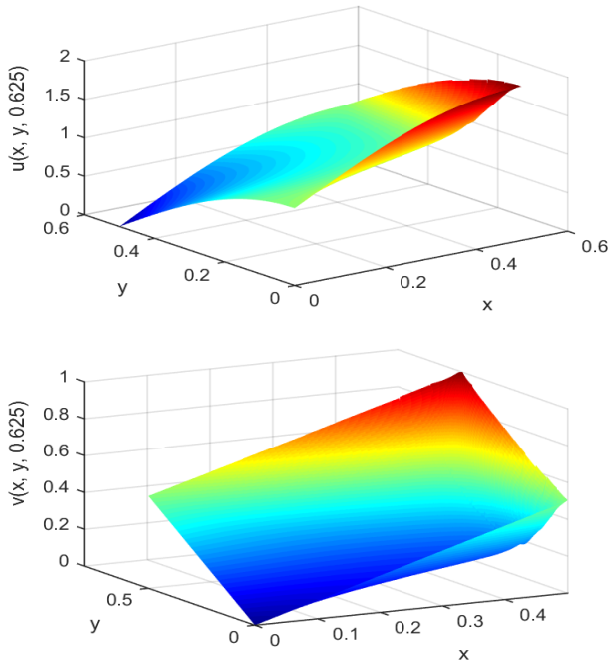

Figure 4: Approximate solutions u and v for Example 3 with $Re = 50$ at $T = 0.625$. The results are reported for $\tau = \sigma = 2$, approximate polynomial of degree two with $h = 0.05$ and $\Delta t = 0.001$.

completely dependent on the fluxes. So, one of the hardships of using the HDG method is finding appropriate definitions of numerical fluxes that guarantee stability. Fortunately, we presented a stable HDG method for solving system (1), while there is no stable (with a proven theorem) LDG method yet. Investigating the convergence of HDG methods for coupled and nonlinear problems is not easy. According to the authors' knowledge, already, the convergence of the HDG methods has been studied just for some simple and linear equations. Convergence of the proposed method can be considered as one of our future works.

The same as other HDG methods, by converting the initial system to a system of first-order equations and defining approximate broken Sobolev spaces associated with spatial partitioning, we set up the semi-discrete variational formulation of the coupled Burgers. Based on the structure of the HDG method, we have proposed numerical traces and fluxes for the variational formulation of the first-order equations. Numerical traces are supposed as global unknowns and depend on Dirichlet boundary data. Defining numerical flux in any HDG method plays a significant role in the stability of the semi-discrete HDG method over a time interval. After introducing appropriate numerical fluxes and imposing sufficient global equations over the spatial partitioning for system (1), the L^2 stability of the proposed semi-discrete HDG methods has been investigated under specific mild conditions on the stabilization parameters that are used in the definitions of numerical fluxes. With the intention of gaining a fully discrete scheme, the Crank–Nicolson method has been applied for time discretization. The choice of the Crank–Nicolson method was because of its unconditional stability and second-order accuracy. To preserve the second order of accuracy in time, the Newton–Raphson method has been nominated for solving the nonlinear system of equations. To solve the large and sparse linear variational systems, which is related to the Newton–Raphson method, the Schur complement idea has been used for reducing computational complexity and designing smaller systems of equations. To explain the details of the HDG method, an algorithm has been prepared. To verify the efficiency of the proposed HDG method, the method was applied to some model problems. In the presented examples, we showed that approximate solutions and their first derivatives of degree k have converged at order $k+1$, which is an optimal order of convergence. Also, in another example, the ability of the proposed HDG method was checked for solving the 2D coupled Burgers equations with different and high Reynolds numbers. Finally, we tested this method to solve a system without the exact solution, and pleasant results were observed. Regarding the flexibility of the method and numeric experiences, one can infer that the HDG method is one of the outstanding methods that has been exploited for various types of evolution problems in higher dimensions.

Appendix

As mentioned in section 4, a fully discrete approximation method is obtained for solving the nonlinear coupled Burgers equations (1) by using the HDG and Crank–Nicolson methods for spatial and temporal discretization, respectively. Regarding the definitions of approximation spaces, the goal is to find $(n, v^n, p_1^n, p_2^n, q_1^n, q_2^n) \in S_{h,k}^6$ and $(\xi^n, \zeta^n) \in M_{h,k}(0, \Gamma_{\mathfrak{u}}) \times M_{h,k}(0, \Gamma_{\mathfrak{v}})$, such that all equations in (6) and (14) are satisfied for $n = 1, 2, \ldots, J$. As stated in section 4, by summing over all elements, inserting the flux definitions (5) into (6) and (14) at the time level t_n and also using boundary conditions (4), the following system of equations is obtained:

$$
\begin{aligned}
&\frac{1}{\Delta t}(u^n, w_1)_{\mathscr{K}_h} + \frac{1}{2}(u^n u_x^n, w_1)_{\mathscr{K}_h} + \frac{1}{2}(v^n u_y^n, w_1)_{\mathscr{K}_h} - \frac{1}{2\mathrm{Re}}(p_{1x}^n, w_1)_{\mathscr{K}_h} \\
&\quad - \frac{1}{2\mathrm{Re}}(p_{2y}^n, w_1)_{\mathscr{K}_h} + \frac{\tau}{2}\langle u^n, w_1\rangle_{\partial\mathscr{K}_h} - \frac{\tau}{2}\langle \xi^n, w_1\rangle_{\partial\mathscr{K}_h\setminus\Gamma_{\mathfrak{u}}} = l_1(w_1), \\
&(p_1^n, w_{11})_{\mathscr{K}_h} + (u^n, (w_{11})_x)_{\mathscr{K}_h} - < \xi^n \mathbf{n}_x, w_{11} >_{\partial\mathscr{K}_h\setminus\Gamma_{\mathfrak{u}}} = l_2(w_{11}), \\
&(p_2^n, w_{12})_{\mathscr{K}_h} + (u^n, (w_{12})_y)_{\mathscr{K}_h} - < \xi^n \mathbf{n}_y, w_{12} >_{\partial\mathscr{K}_h\setminus\Gamma_{\mathfrak{u}}} = l_3(w_{12}), \\
&\frac{1}{\Delta t}(v^n, w_2)_{\mathscr{K}_h} + \frac{1}{2}(u^n v_x^n, w_2)_{\mathcal{K}} + \frac{1}{2}(v^n v_y^n, w_2)_{\mathscr{K}_h} - \frac{1}{2\mathrm{Re}}(q_{1x}^n, w_2)_{\mathscr{K}_h} \\
&\quad - \frac{1}{2\mathrm{Re}}(q_{2y}^n, w_2)_{\mathscr{K}_h} + \frac{\sigma}{2}\langle v^n, w_2\rangle_{\partial\mathscr{K}_h} - \frac{\sigma}{2}\langle \zeta^n, w_2\rangle_{\partial\mathscr{K}_h\setminus\Gamma_{\mathfrak{v}}} = l_4(w_2), \\
&(q_1^n, w_{21})_{\mathscr{K}_h} + (v^n, (w_{21})_x)_{\mathscr{K}_h} - < \zeta^n \mathbf{n}_x, w_{21} >_{\partial\mathscr{K}_h\setminus\Gamma_{\mathfrak{v}}} = l_5(w_{21}), \\
&(q_2^n, w_{22})_{\mathscr{K}_h} + (v^n, (w_{22})_y)_{\mathscr{K}_h} - < \zeta^n \mathbf{n}_y, w_{22} >_{\partial\mathscr{K}_h\setminus\Gamma_{\mathfrak{v}}} = l_6(w_{22}), \\
&\tau\langle u^n, \mu_1\rangle_{\partial\mathscr{K}_h\setminus\mathcal{F}_h^\partial} - \tau\langle \xi^n, \mu_1\rangle_{\partial\mathscr{K}_h\setminus\mathcal{F}_h^\partial} - \frac{1}{\mathrm{Re}}\langle p_1^n \mathbf{n}_x, \mu_1\rangle_{\partial\mathscr{K}_h} \\
&\qquad - \tfrac{1}{\mathrm{Re}}\langle p_2^n \mathbf{n}_y, \mu_1\rangle_{\partial\mathscr{K}_h} = 0, \\
&\sigma\langle v^n, \mu_2\rangle_{\partial\mathscr{K}_h\setminus\mathcal{F}_h^\partial} - \sigma\langle \zeta^n, \mu_2\rangle_{\partial\mathscr{K}_h\setminus\mathcal{F}_h^\partial} - \frac{1}{\mathrm{Re}}\langle q_1^n \cdot \mathbf{n}_x, \mu_2\rangle_{\partial\mathscr{K}_h} \\
&\qquad - \tfrac{1}{\mathrm{Re}}\langle q_2^n \cdot \mathbf{n}_y, \mu_2\rangle_{\partial\mathscr{K}_h} = 0,
\end{aligned}
\tag{19}
$$

where $\mathbf{n} = (\mathbf{n}_x, \mathbf{n}_y)^\intercal$, $\mu_1 \in M_{h,k}^{\mathfrak{u}}(0)$, $\mu_2 \in M_{h,k}^{\mathfrak{v}}(0)$, and

$$
\begin{aligned}
l_1(w) = &\frac{1}{\Delta t}(u^{n-1}, w)_{\mathscr{K}_h} - \frac{1}{2}(u^{n-1}u_x^{n-1}, w)_{\mathscr{K}_h} - \frac{1}{2}(v^{n-1}u_y^{n-1}, w)_{\mathscr{K}_h} \\
&+ \frac{1}{2\mathrm{Re}}(P_{1x}^{n-1}, w_1)_{\mathscr{K}_h} + \frac{1}{2\mathrm{Re}}(P_{2y}^{n-1}, w_1)_{\mathscr{K}_h} - \frac{\tau}{2}\langle u^{n-1}, w\rangle_{\partial\mathscr{K}_h} \\
&+ \frac{\tau}{2}\langle \hat{u}^{n-1}, w\rangle_{\partial\mathscr{K}_h} + \frac{\tau}{2}\langle b_{\mathfrak{u}}^n, w\rangle_{\partial\mathscr{K}_h\cap\Gamma_{\mathfrak{u}}}
\end{aligned}
$$

$$
\begin{aligned}
l_4(w) = &\frac{1}{\Delta t}(v^{n-1}, w)_{\mathscr{K}_h} - \frac{1}{2}(u^{n-1}v_x^{n-1}, w)_{\mathscr{K}_h} - \frac{1}{2}(v^{n-1}v_y^{n-1}, w)_{\mathscr{K}_h} \\
&+\frac{1}{2\mathrm{Re}}(q_{1x}^{n-1}, w)_{\mathscr{K}_h} + \frac{1}{2\mathrm{Re}}(q_{2y}^{n-1}, w)_{\mathscr{K}_h} - \frac{\sigma}{2}\langle v^{n-1}, w\rangle_{\partial\mathscr{K}_h} \\
&+\frac{\sigma}{2}\langle \hat{v}^{n-1}, w_1\rangle_{\partial\mathscr{K}_h} + \frac{\sigma}{2}\langle b_{\mathfrak{v}}^n, w\rangle_{\partial\mathscr{K}_h\cap\Gamma_{\mathfrak{v}}}
\end{aligned}
$$

$$
l_2(w) = \langle b_{\mathfrak{u}}^n \mathbf{n}_x, w\rangle_{\partial\mathscr{K}_h\cap\Gamma_{\mathfrak{u}}}, \qquad l_3(w) = \langle b_{\mathfrak{u}}^n \mathbf{n}_y, w\rangle_{\partial\mathscr{K}_h\cap\Gamma_{\mathfrak{u}}},
$$

$$
l_5(w) = \langle b_{\mathfrak{v}}^n \mathbf{n}_x, w\rangle_{\partial\mathscr{K}_h\cap\Gamma_{\mathfrak{v}}}, l_6(w) = \langle b_{\mathfrak{v}}^n \mathbf{n}_y, w\rangle_{\partial\mathscr{K}_h\cap\Gamma_{\mathfrak{v}}}.
$$

Regarding to the nonlinear weak formulation (19), it is needed to convert this weak form to a linear variational form by a suitable iterative method. As explained in section 4, by applying the Newton–Raphson method to the nonlinear variational formulation (19), we intend to find

$$
\delta W_{n,i} = (\delta u_{n,i}, \delta v_{n,i}, \delta p_{1,n,i}, \delta p_{2,n,i}, \delta q_{1,n,i}, \delta q_{2,n,i}, \delta\xi_{n,i}, \delta\zeta_{n,i}),
$$

such that for all $(w_1, w_2, w_{11}, w_{12}, w_{21}, w_{22}) \in S_{h,k}^6$ and $(\mu_1, \mu_2) \in M_{h,k}(0, \Gamma_{\mathfrak{u}})\times M_{h,k}(0, \Gamma_{\mathfrak{v}})$, the bilinear form system (15) holds. We finish the Appendix by defining all multilinear forms and linear functionals, which are considered in (15),

$$
\begin{aligned}
\tilde{\mathsf{a}}_1(\delta u_{n,i}, w) =&\frac{1}{\Delta t}(\delta u_{n,i}, w)_{\mathscr{K}_h} + \frac{1}{2}((u_x)_{n,i-1}\delta u_{n,i}, w)_{\mathscr{K}_h} \\
&+ \frac{1}{2}(u_{n,i-1}(\delta u_x)_{n,i}, w)_{\mathscr{K}_h} + \frac{\tau}{2}\langle \delta u_{n,i}, w\rangle_{\partial\mathscr{K}_h} \\
&+ \frac{1}{2}(v_{n,i-1}\delta(u_y)_{n,i}, w)_{\mathscr{K}_h}, \\
\tilde{\mathsf{a}}_2(\delta v_{n,i}, w) =&\frac{1}{2}((u_y)_{n,i-1}\delta v_{n,i}, w)_{\mathscr{K}_h}, \\
\tilde{\mathsf{a}}_3(\delta p_{1,n,i}, w) =& -\frac{1}{2\mathrm{Re}}((\delta p_{1,n,i})_x, w)_{\mathscr{K}_h}, \\
\tilde{\mathsf{a}}_4(\delta p_{2,n,i}, w) =& -\frac{1}{2\mathrm{Re}}((\delta p_{2,n,i})_x, w)_{\mathscr{K}_h}, \\
\tilde{\mathsf{a}}_5(\delta\xi_{n,i}, w) =& -\frac{\tau}{2}\langle \delta\xi_{n,i}, w\rangle_{\partial\mathscr{K}_h\setminus\Gamma_{\mathfrak{u}}}, \\
\tilde{\mathsf{b}}_1(\delta u_{n,i}, w) =&(\delta u_{n,i}, w_x)_{\mathscr{K}_h}, \\
\tilde{\mathsf{b}}_2(\delta p_{1,n,i}, w) =&(\delta p_{1,n,i}, w)_{\mathscr{K}_h}, \\
\tilde{\mathsf{b}}_4(\delta u_{n,i}, w) =&(\delta u_{n,i}, \mathbf{w}_y)_{\mathscr{K}_h}, \\
\tilde{\mathsf{b}}_3(\delta\xi_{n,i}\mathbf{n}, w) =& -\langle \delta\xi_{n,i}\mathbf{n}_x, w\rangle_{\partial\mathscr{K}_h\setminus\Gamma_{\mathfrak{u}}}, \\
\tilde{\mathsf{b}}_5(\delta\xi_{n,i}, w) =& -\langle \delta\xi_{n,i}\mathbf{n}_y, w\rangle_{\partial\mathscr{K}_h\setminus\Gamma_{\mathfrak{u}}}, \\
\tilde{\mathsf{c}}_2(\delta v_{n,i}, w) =&\frac{1}{\Delta t}(\delta v_{n,i}, w)_{\mathscr{K}_h} + \frac{1}{2}((v_y)_{n,i-1}\delta v_{n,i}, w)_{\mathscr{K}_h}
\end{aligned}
$$

$$
\begin{aligned}
&+\frac{1}{2}(u_{n,i-1}\delta(v_x)_{n,i},w)_{\mathscr{K}_h}+\frac{\sigma}{2}\langle\delta v_{n,i},w\rangle_{\partial\mathscr{K}_h}\\
&+\frac{1}{2}(v_{n-1,i}(\delta v_y)_{n,i},w)_{\mathscr{K}_h},\\
\tilde{\mathsf{c}}_1(\delta u_{n,i},w)=&\frac{1}{2}((v_x)_{n,i-1}\delta u_{n,i},w)_{\mathscr{K}_h},\\
\tilde{\mathsf{c}}_3(\delta q_{1,n,i},w)=&-\frac{1}{2\mathrm{Re}}((\delta p_{1,n,i})_x,w)_{\mathscr{K}_h},\\
\tilde{\mathsf{c}}_4(\delta q_{2,n,i},w)=&-\frac{1}{2\mathrm{Re}}((\delta q_{2,n,i})_x,w)_{\mathscr{K}_h},\\
\tilde{\mathsf{c}}_5(\delta\zeta_{n,i},w)=&-\frac{\sigma}{2}\langle\delta\zeta_{n,i},w\rangle_{\partial\mathscr{K}_h\setminus\Gamma_{\mathfrak{v}}}\\
\tilde{\mathsf{d}}_1(\delta u_{n,i},\mu)=&\langle\delta u_{n,i},\mu\rangle_{\partial\mathscr{K}_h\setminus\mathcal{F}_h^{\partial}},\\
\tilde{\mathsf{d}}_2(\delta p_{1,n,i},\mu)=&-\frac{1}{\mathrm{Re}}\langle\delta p_{1,n,i}\mathbf{n}_x,\mu\rangle_{\partial\mathscr{K}_h},\\
\tilde{\mathsf{d}}_3(\delta p_{2,n,i},\mu)=&-\frac{1}{\mathrm{Re}}\langle\delta p_{2,n,i}\mathbf{n}_y,\mu\rangle_{\partial\mathscr{K}_h},\\
\tilde{\mathsf{d}}_4(\delta\xi_{n,i},\mu)=&\langle\delta\xi_{n,i},\mu\rangle_{\partial\mathscr{K}_h\setminus\mathcal{F}_h^{\partial}},\\
\tilde{\mathsf{l}}_1(w)=&\frac{1}{\Delta t}(u^{n-1},w)_{\mathscr{K}_h}-\frac{1}{2}(u^{n-1}u_x^{n-1},w)_{\mathscr{K}_h}-\frac{1}{2}(v^{n-1}u_y^{n-1},w)_{\mathscr{K}_h}\\
&+\frac{1}{2\mathrm{Re}}(P_{1x}^{n-1},w_1)_{\mathscr{K}_h}+\frac{1}{2\mathrm{Re}}(P_{2y}^{n-1},w_1)_{\mathscr{K}_h}-\frac{\tau}{2}\langle u^{n-1},w\rangle_{\partial\mathscr{K}_h}\\
&+\frac{\tau}{2}\langle\hat{u}^{n-1},w\rangle_{\partial\mathscr{K}_h}+\frac{\tau}{2}\langle b_{\mathfrak{u}}^n,w\rangle_{\partial\mathscr{K}_h\cap\Gamma_{\mathfrak{u}}}-\frac{1}{\Delta t}(u_{n,i-1},w)_{\mathscr{K}_h}\\
&-\frac{1}{2}(u_{n,i-1}p_{1,n,i-1},w)_{\mathscr{K}_h}-\frac{1}{2}(v_{n,i-1}p_{2,n,i-1},w)_{\mathscr{K}_h}\\
&+\frac{1}{2\mathrm{Re}}((p_{1,n,i-1})_x,w)_{\mathscr{K}_h}+\frac{1}{2\mathrm{Re}}((p_{2,n,i-1})_y,w)_{\mathscr{K}_h}\\
&-\frac{\tau}{2}\langle u_{n,i-1},w\rangle_{\partial\mathscr{K}_h}+\frac{\tau}{2}\langle\xi_{n,i-1},w\rangle_{\partial\mathscr{K}_h\setminus\Gamma_{\mathfrak{u}}},\\
\tilde{\mathsf{l}}_2(w)=&\langle b_{\mathfrak{u}}^n\mathbf{n}_x,w\rangle_{\partial\mathscr{K}_h\cap\Gamma_{\mathfrak{u}}}-(p_{1,n,i-1},w)_{\mathscr{K}_h}-(u_{n,i-1},(w)_x)_{\mathscr{K}_h}\\
&+<\xi_{n,i-1}\mathbf{n}_x,w>_{\partial\mathscr{K}_h\setminus\Gamma_{\mathfrak{u}}},\\
\tilde{\mathsf{l}}_3(w)=&\langle b_{\mathfrak{u}}^n\mathbf{n}_y,w\rangle_{\partial\mathscr{K}_h\cap\Gamma_{\mathfrak{u}}}-(p_{2,n,i-1},w)_{\mathscr{K}_h}-(u_{n,i-1},(w)_y)_{\mathscr{K}_h}\\
&+<\xi_{n,i-1}\mathbf{n}_y,w>_{\partial\mathscr{K}_h\setminus\Gamma_{\mathfrak{u}}},\\
\tilde{\mathsf{l}}_4(w)=&\frac{1}{\Delta t}(v^{n-1},w)_{\mathscr{K}_h}-\frac{1}{2}(u^{n-1}v_x^{n-1},w)_{\mathscr{K}_h}-\frac{1}{2}(v^{n-1}v_y^{n-1},w)_{\mathscr{K}_h}\\
&+\frac{1}{2\mathrm{Re}}(q_{1x}^{n-1},w_1)_{\mathscr{K}_h}+\frac{1}{2\mathrm{Re}}(q_{2y}^{n-1},w_1)_{\mathscr{K}_h}-\frac{\sigma}{2}\langle q^{n-1},w\rangle_{\partial\mathscr{K}_h}\\
&+\frac{\sigma}{2}\langle\hat{v}^{n-1},w\rangle_{\partial\mathscr{K}_h}+\frac{\sigma}{2}\langle b_{\mathfrak{v}}^n,w\rangle_{\partial\mathscr{K}_h\cap\Gamma_{\mathfrak{v}}}-\frac{1}{\Delta t}(v_{n,i-1},w)_{\mathscr{K}_h}\\
&-\frac{1}{2}(u_{n,i-1}q_{1,n,i-1},w)_{\mathscr{K}_h}-\frac{1}{2}(v_{n,i-1}q_{2,n,i-1},w)_{\mathscr{K}_h}
\end{aligned}
$$

$$
\begin{aligned}
&+\frac{1}{2\mathrm{Re}}((q_{1,n,i-1})_x,w)_{\mathscr{K}_h}+\frac{1}{2\mathrm{Re}}((q_{2,n,i-1})_y,w)_{\mathscr{K}_h}\\
&-\frac{\sigma}{2}\langle v_{n,i-1},w\rangle_{\partial\mathscr{K}_h}+\frac{\sigma}{2}\langle\zeta_{n,i-1},w\rangle_{\partial\mathscr{K}_h\setminus\Gamma_{\mathfrak{v}}},\\
\tilde{\mathrm{I}}_5(w)=&\langle b_{\mathfrak{v}}^n\mathbf{n}_x,w\rangle_{\partial\mathscr{K}_h\cap\Gamma_{\mathfrak{v}}}-(q_{1,n,i-1},w)_{\mathscr{K}_h}-(v_{n,i-1},(w)_x)_{\mathscr{K}_h}\\
&+<\zeta_{n,i-1}\mathbf{n}_x,w>_{\partial\mathscr{K}_h\setminus\Gamma_{\mathfrak{v}}},\\
\tilde{\mathrm{I}}_6(w)=&\langle b_{\mathfrak{v}}^n\mathbf{n}_y,w\rangle_{\partial\mathscr{K}_h\cap\Gamma_{\mathfrak{v}}}-(q_{2,n,i-1},w)_{\mathscr{K}_h}-(v_{n,i-1},(w)_y)_{\mathscr{K}_h}\\
&+<\zeta_{n,i-1}\mathbf{n}_y,w>_{\partial\mathscr{K}_h\setminus\Gamma_{\mathfrak{v}}},\\
\tilde{\mathrm{I}}_7(\mu)=&-\tau\langle u_{n,i-1},\mu\rangle_{\partial\mathscr{K}_h\setminus\mathcal{F}_h^{\partial}}+\tau\langle\xi_{n,i-1},\mu\rangle_{\partial\mathscr{K}_h\setminus\mathcal{F}_h^{\partial}}\\
&+\frac{1}{\mathrm{Re}}\langle p_{1,n,i-1}\mathbf{n}_x,\mu\rangle_{\partial\mathscr{K}_h}+\frac{1}{\mathrm{Re}}\langle p_{2,n,i-1}\mathbf{n}_y,\mu\rangle_{\partial\mathscr{K}_h},\\
\tilde{\mathrm{I}}_8(\mu)=&-\sigma\langle v_{n,i-1},\mu\rangle_{\partial\mathscr{K}_h\setminus\mathcal{F}_h^{\partial}}+\sigma\langle\zeta_{n,i-1},\mu\rangle_{\partial\mathscr{K}_h\setminus\mathcal{F}_h^{\partial}}\\
&+\frac{1}{\mathrm{Re}}\langle q_{1,n,i-1}\mathbf{n}_x,\mu\rangle_{\partial\mathscr{K}_h}+\frac{1}{\mathrm{Re}}\langle q_{2,n,i-1}\mathbf{n}_y,\mu\rangle_{\partial\mathscr{K}_h}.
\end{aligned}
$$

References

[1] Adomian, G. *The diffusion-Brusselator equation*, Comput. Math. with Appl. **29(5)** (1995), 1–3.

[2] Aliyi Koroche, K. and Muleta Chemeda, H. *Sixth-order compact finite difference method for solving KDV-Burger equation in the application of wave propagations*, Iran. J. Numer. Anal. Optim. 12(2) (2022), 277–300.

[3] Bahadır, A.R. *A fully implicit finite-difference scheme for two-dimensional Burgers' equations*, Appl. Math. Comput. 137(1) (2003), 131–137.

[4] Baharloui, S., Mokhtari, R. and Chegini, N. *A stable numerical scheme based on the hybridized discontinuous Galerkin method for the Ito-type coupled KdV system*, Commun. Appl. Math. Comput. 4(4) (2022), 1351–1373.

[5] Burgers, J.M. *A mathematical model illustrating the theory of turbulence*, Adv. Appl. Mech. (1948), 171–199.

[6] Castillo, P. *A review of the local discontinuous Galerkin (LDG) method applied to elliptic problems*, Appl. Numer. Math. 56(10-11) (2006), 1307–1313.

[7] Castillo, P. and Gómez, S. *Conservative super-convergent and hybrid discontinuous Galerkin methods applied to nonlinear Schrödinger equations*, Appl. Math. Comput. 371 (2020), 124950.

[8] Chand, A. and Saha Ray, S. *Numerical simulation of Allen–Cahn equation with nonperiodic boundary conditions by the local discontinuous Galerkin method*, Int. J. Mod. Phys. B. 37(02) (2023), 2350019.

[9] Cockburn, B., Fu, G. and Qiu, W. *A note on the devising of superconvergent HDG methods for Stokes flow by M-decompositions*, IMA J. Numer. Anal. 37(2) (2017), 730–749.

[10] Cockburn, B., Hou, S. and Shu, C.W. *The Runge-Kutta local projection discontinuous Galerkin finite element method for conservation laws. IV. The multidimensional case*, Math. Comput. 54(190) (1990), 545–581.

[11] Cockburn, B. and Gopalakrishnan, J. *A characterization of hybridized mixed methods for second order elliptic problems*, SIAM J. Numer. Anal. 42(1) (2004), 283–301.

[12] Cockburn, B., Gopalakrishnan, J. and Lazarov, R. *Unified hybridization of discontinuous Galerkin, mixed, and continuous Galerkin methods for second order elliptic problems*, SIAM J. Numer. Anal. 47(2) (2009), 1319–1365.

[13] Cockburn, B., Gopalakrishnan, J. and Sayas, F.J. *A projection-based error analysis of HDG methods*, Math. Comput. 79(271) (2010), 1351–1367.

[14] Cockburn, B., Guzmán, J., Soon, S.C. and Stolarski, H.K. *An analysis of the embedded discontinuous Galerkin method for second-order elliptic problems*, SIAM J. Numer. Anal. 47(4) (2009), 2686–2707.

[15] Cockburn, B. and Shu, C.W. *The local discontinuous Galerkin method for time-dependent convection-diffusion systems*, SIAM J. Numer. Anal. 35(6) (1998), 2440–2463.

[16] Cockburn, B. and Shu, C.W. *The Runge-Kutta discontinuous Galerkin method for conservation laws V: multidimensional systems*, J. Comput. Phys. 141(2) (1998), 199–224.

[17] Cole, J.D. *On a quasi-linear parabolic equation occurring in aerodynamics*, Q. Appl. Math. 9(3) (1951), 225-236.

[18] Debnath, L. *Nonlinear partial differential equations for scientists and engineers*, Third edition. Birkhäuser/Springer, New York, 2012.

[19] El-Sayed, S.M. and Kaya, D. *On the numerical solution of the system of two-dimensional Burgers' equations by the decomposition method*, Appl. Math. Comput. 158(1) (2004), 101–109.

[20] Fletcher, C.A. *Generating exact solutions of the two-dimensional Burgers' equations*, Int. J. Numer. Methods Fluids. 3 (1983), 213–216.

[21] Giacomini, M., Karkoulias, A., Sevilla, R. and Huerta, A. *A superconvergent HDG method for Stokes flow with strongly enforced symmetry of the stress tensor*, J. Sci. Comput. 77(3) (2018), 1679–1702.

[22] Giacomini, M., Sevilla, R. and Huerta, A. *Tutorial on Hybridizable Discontinuous Galerkin (HDG) formulation for incompressible flow problems*, Modeling in Engineering Using Innovative Numerical Methods for Solids and Fluids, (2020), 163–201.

[23] Khater, A.H., Temsah, R.S. and Hassan, M. *A Chebyshev spectral collocation method for solving Burgers'-type equations*, J. Comput. Appl. Math. 222(2) (2008), 333–350.

[24] Kumar, V., Singh, S. and Koksal, M.E. *A composite algorithm for numerical solutions of two-dimensional coupled Burgers equations*, J. Math. (2021), 1–13.

[25] Ling, D., Shu, C.W. and Yan, W. *Local discontinuous Galerkin methods for diffusive-viscous wave equations*, J. Comput. Appl. Math. 419 (2023), 114690.

[26] Logan, J.D. *An introduction to nonlinear partial differential equations*, John Wiley and Sons (2008).

[27] Mokhtari, R. and Mohseni, M. *A meshless method for solving mKdV equation*, Comput. Phys. Commun. 183(6) (2012), 1259–1268.

[28] Mokhtari, R., Toodar, A.S. and Chegini, N.G. *Application of the generalized differential quadrature method in solving Burgers' equations*, Commun. Theor. Phys. 56(6) (2011), 1009.

[29] Nguyen, N.C. and Peraire, J. *Hybridizable discontinuous Galerkin methods for partial differential equations in continuum mechanics*, J. Comput. Phys. 231(18) (2012), 5955–5988.

[30] Peraire, J., Nguyen, N. and Cockburn, B. *A hybridizable discontinuous Galerkin method for the compressible Euler and Navier-Stokes equations*, In 48th AIAA aerospace sciences meeting including the new horizons forum and aerospace exposition, 363 (2010).

[31] Rong-Pei, Z., Xi-Jun, Y. and Guo-Zhong, Z. *Local discontinuous Galerkin method for solving Burgers and coupled Burgers equations*, Chin. Phys. B. 20(11) (2011), 110205.

[32] Sevilla, R., Giacomini, M., Karkoulias, A. and Huerta, A. *A superconvergent hybridisable discontinuous Galerkin method for linear elasticity*, Int. J. Numer. Methods Eng. 116(2) (2018), 91–116.

[33] Sevilla, R. and Huerta, A. *Tutorial on hybridizable discontinuous Galerkin (HDG) for second-order elliptic problems*, Advanced Finite Element Technologies, (2016), 105–129.

[34] Shin, D., Jeon, Y. and Park, E.J. *Analysis of hybrid discontinuous Galerkin methods for linearized Navier–Stokes equations*, Numer. Methods Partial Differ. Equ. 39(1) (2023), 304–328.

[35] Srivastava, V.K. and Tamsir, M. *Crank-Nicolson semi implicit approach for numerical solutions of two-dimensional coupled nonlinear Burgers' equations*, Int. J. Appl.Mech. 17(2) (2012), 571.

[36] Vila-Pérez, J., Giacomini, M., Sevilla, R. and Huerta, A. *Hybridisable discontinuous Galerkin formulation of compressible flows*, Arch. Comput. Methods Eng. 28(2) (2021), 753–784.

[37] Williams, D. *An entropy stable, hybridizable discontinuous Galerkin method for the compressible Navier-Stokes equations*, Math. Comput. 87(309) (2018), 95–121.

[38] Yang, X., Ge, Y. and Lan, B. *A class of compact finite difference schemes for solving the 2D and 3D Burgers' equations*, Math. Comput. Simul. 185 (2021), 510–534.

[39] Zogheib, B., Tohidi, E., Baskonus, H.M. and Cattani, C. *Method of lines for multi-dimensional coupled viscous Burgers' equations via nodal Jacobi spectral collocation method*, Phys. Scr. 96(12) (2021), 124011.

How to cite this article
Baharlouei, S., Mokhtari, R. and Chegini, N., Solving two-dimensional coupled Burgers equations via a stable hybridized discontinuous Galerkin method. *Iran. j. numer. anal. optim.*, 2023; 13(3): 397-425. https://doi.org/10.22067/ijnao.2023.80916.1215